Taylor & Francis
Taylor & Francis Group

REPORT

🔓 OPEN ACCESS | Check for updates

IL-2-armored peptide-major histocompatibility class I bispecific antibodies redirect antiviral effector memory CD8+ T cells to induce potent anti-cancer cytotoxic activity with limited cytokine release

John S. Schardt[a]*, Even Walseng[a]*, Kim Le[a], Chunning Yang[a], Pooja Shah[a], Ying Fu[a], Kausar Alam[a], Cathryn R. Kelton[b], Yu Gu[a], Fengying Huang[a], Jia Lin[a], Wenhai Liu[a], Andrew Dippel[a], Hanzhi Zhang[a], Kathy Mulgrew[b], Stacy Pryts[b], Vijaykumar Chennupati[c], Hung-Chang Chen[c], Jessica Denham[d], Xiaoru Chen[d], Pallab Pradhan[d], Yuling Wu[d], Colin Hardman[e], Chihao Zhao[a], Michael Kierny[a], Yang Song[a], Simon J. Dovedi[c], Saso Cemerski[b], and Yariv Mazor[a]

[a]R&D Biologics Engineering, AstraZeneca, Gaithersburg, MD, USA; [b]Oncology ICC, AstraZeneca, Gaithersburg, MD, USA; [c]Data Science and Advanced Analytics, AstraZeneca, Gaithersburg, MD, USA; [d]Oncology ICC, AstraZeneca, Cambridge, UK; [e]Discovery Bioanalysis, Clinical Pharmacology & Safety Sciences (CPSS), R&D, AstraZeneca, Gaithersburg, MD, USA

ABSTRACT

T cell engagers (TCEs) are becoming an integral class of biological therapeutic owing to their highly potent ability to eradicate cancer cells. Nevertheless, the widespread utility of classical CD3-targeted TCEs has been limited by narrow therapeutic index (TI) linked to systemic CD4+ T cell activation and aberrant cytokine release. One attractive approach to circumvent the systemic activation of pan CD3+ T cells and reduce the risk of cytokine release syndrome is to redirect specific subsets of T cells. A promising strategy is the use of peptide-major histocompatibility class I bispecific antibodies (pMHC-IgGs), which have emerged as an intriguing modality of TCE, based on their ability to selectively redirect highly reactive viral-specific effector memory cytotoxic CD8+ T cells to eliminate cancer cells. However, the relatively low frequency of these effector memory cells in human peripheral blood mononuclear cells (PBMCs) may hamper their redirection as effector cells for clinical applications. To mitigate this potential limitation, we report here the generation of a pMHC-IgG derivative known as guided-pMHC-staging (GPS) carrying a covalent fusion of a monovalent interleukin-2 (IL-2) mutein (H16A, F42A). Using an anti-epidermal growth factor receptor (EGFR) arm as a proof-of-concept, tumor-associated antigen paired with a single-chain HLA-A *02:01/CMVpp65 pMHC fusion moiety, we demonstrate *in vitro* that the IL-2-armored GPS modality robustly expands CMVpp65-specific CD8+ effector memory T cells and induces potent cytotoxic activity against target cancer cells. Similar to GPS, IL-2-armored GPS molecules induce modulated T cell activation and reduced cytokine release profile compared to an analogous CD3-targeted TCE. *In vivo* we show that IL-2-armored GPS, but not the corresponding GPS, effectively expands grafted CMVpp65 CD8+ T cells from unstimulated human PBMCs in an NSG mouse model. Lastly, we demonstrate that the IL-2-armored GPS modality exhibits a favorable developability profile and monoclonal antibody-like pharmacokinetic properties in human neonatal Fc receptor transgenic mice. Overall, IL-2-armored GPS represents an attractive approach for treating cancer with the potential for inducing vaccine-like antiviral T cell expansion, immune cell redirection as a TCE, and significantly widened TI due to reduced cytokine release.

Introduction

T cell engagers (TCEs), which are a class of biologic drugs that mediate the formation of functional immunological synapses between T cells and cancer cells to trigger cancer cell death, represent a promising strategy for the treatment of cancer, with several TCEs having received FDA approval for treating hematological and solid malignancies.[1–4] While TCEs are attractive cancer therapeutics based on their potent ability to eliminate cancer cells, the widespread clinical translation of TCEs has been limited.

A primary challenge obstructing TCE clinical translation is narrow TI in which tolerable dosing is restricted by side effects such as cytokine release syndrome. Conventional TCEs typically function via simultaneous engagement of CD3 on the T cell surface and tumor-associated antigen (TAA) on the cancer cell surface. This reliance on the engagement of CD3 to bind and activate T cells may be suboptimal considering that CD3 is expressed on all T cells, contributing to pan T cell activation, elevated cytokine release linked to CD4+ T cell activation, and exacerbation of immunosuppression linked to regulatory T cell (Treg) activation (Figure 1).[5] While shifting paradigms for preclinical and clinical dose optimization are anticipated to address this issue in part,[6] novel strategies with the potential for a broader and deeper TI are needed to address
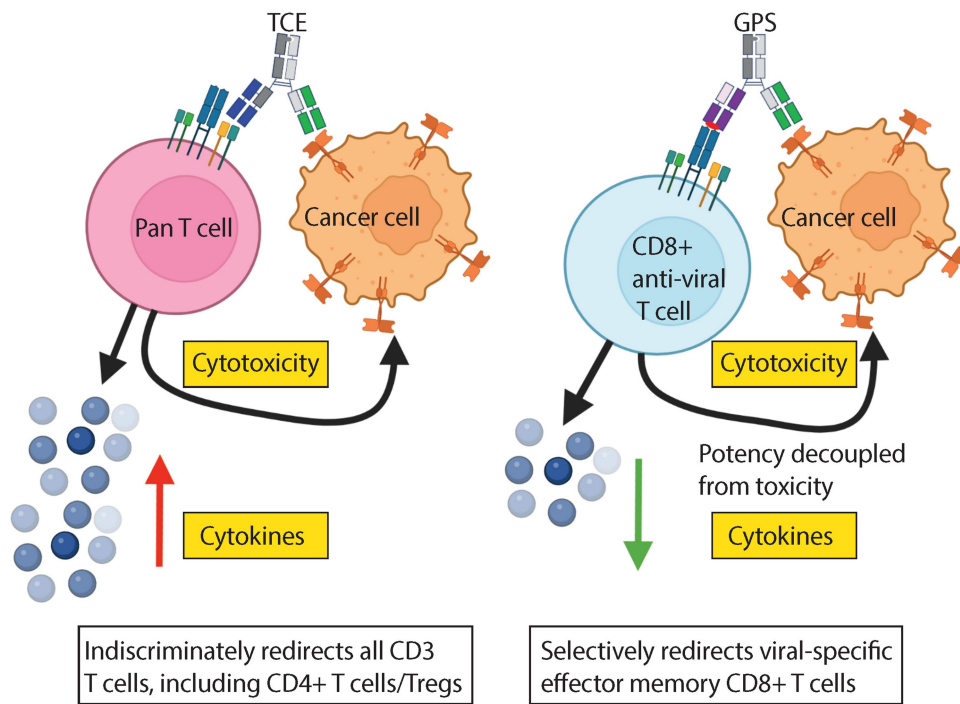
Figure 1. GPS engages virus-specific effector, memory CD8+ T cells to induce potent cytotoxic activity against target tumor cells with reduced risk of cytokine-associated toxicity Conventional TCEs engage CD3 expressed on all T cells, increasing the risk for aberrant cytokine release associated with pan T cell activation. GPS selectively engage with virus-specific effector memory CD8+ T cells toward maintaining potent cytotoxic activity with reduced risk of cytokine release syndrome associated with CD4+ T cell activation.

the significant unmet clinical need for safe and effective cancer treatment.

One strategy used across several platforms and over a range of targets to address the narrow TI associated with TCEs is the use of affinity optimized variants of the anti-CD3 moiety.[7–9] In particular, TCEs carrying affinity attenuated anti-CD3 domains were shown to achieve similar levels of efficacy as non-optimized anti-CD3 sequences, but exhibited reduced toxicity, peripheral cytokine release, and Treg activation, resulting in an improved TI.[7–9] Previous investigations also highlight the importance of affinity co-optimization of the anti-TAA arm in addition to the anti-CD3 arm to improve TI.[7–9] In particular, Poussin et al. identified that the parameter of TAA density is an important consideration when co-optimizing multispecific TCE affinities. In their study, the authors observed that both anti-TAA and anti-CD3 affinity significantly impact TCE potency in the context of low cell-surface density receptor targets, whereas anti-TAA affinity alone predominantly impacts TCE potency for high-density receptor targets. Beyond affinity optimization, the unique epitopes of the CD3 and TAA arms, molecular format, and the modality pharmacokinetics (PK) have also been identified as important factors influencing TCE activity and TI.[10,11] Overall, molecular engineering and optimization principles have broadly improved the design of TCEs for clinical translation.

Another innovative strategy to mitigate the challenge of narrow TI associated with conventional CD3 TCEs is the selective recruitment and redirection of virus-specific memory bystander T cells for selective killing of target cancer cells.[12–20] The redirection of these virus-specific effector memory CD8+ T cells is motivated by the remarkable properties of antiviral cells in

terms of surveillance breadth across tissues, resistance to exhaustion and the capacity for innate and adaptive anti-tumor immune responses.[12–16] In particular, Rosato et al. identified the consistent presence of antiviral T cells, including cytomegalovirus (CMV), Epstein-Barr virus (EBV), and influenza, within human tumor tissues, such as cancers of the breast, head and neck, brain, and uterus. They observed that detection of antiviral cells in the blood was fully predictive of their presence within the tumor microenvironment (TME), which ranged from less than 1% to 10% of total CD8+ T cells in the TME.[12] Moreover, the authors demonstrated that mimicking viral infection via intratumoral delivery of viral peptides in mice elicited broad anti-cancer immune responses and tumor growth arrest. Other important research in the field from *Schuessler* et al. highlights the deployment of CMV-specific T cells as an autologous T cell therapy for treating recurrent glioblastoma.[12] Overall, differentiated CD8+ anti-viral bystander cells have demonstrated excellent functionality as rapid and durable cytotoxic effector cells.[17–20]

Building upon these findings, the use of TCEs to selectively redirect antiviral cells has recently emerged as a potential therapeutic approach (Figure 1).[17–20] Preclinical research using peptide-major histocompatibility class I (pMHC) IgG-based TCEs serves a foundational role in informing next-generation approaches to harness and re-direct antiviral effector memory T cells for treating cancer.[17–21] Schmittnaegel et al. investigated the fundamental question as to whether the low frequency of endogenous CMV-reactive T cells was sufficient to confer potent cytotoxic activity.[17–20] Interestingly, the authors reported that pMHC IgGs induced potent *in vitro* cytotoxic activity despite the low frequency of CMV-reactive effector memory cells among non-expanded peripheral blood

mononuclear cells (PBMCs) effector cells (~3% or less among CD8+ T cells), suggesting the re-direction of these anti-viral cells as highly efficient serial killers.[18] Nevertheless, *in vivo* efficacy in mouse models has thus far required *ex vivo* pre-expansion or vaccination to significantly increase the frequency of anti-viral effector cells and achieve significant tumor burden reduction. Collectively, these findings indicate that anti-viral effector memory cell expansion is likely a critical challenge in the translation of pMHC IgGs as effective TCEs.[18,19] To address this limitation, we sought to develop a simple, one-molecule biologics approach with the potential to locally expand anti-viral cells within the TME and re-direct these effector cells to potently eliminate cancer. Given the well-established biological role of interleukin-2 (IL-2) for the activation and expansion of antiviral T cells[22] and the clear clinical utility of this cytokine and its engineered variants,[23] we posited that the incorporation of an engineered IL-2 moiety via covalent fusion to pMHC IgG may be suitable to promote antiviral effector memory cell expansion.

In this study, we report the generation, optimization, and early-stage evaluation of an IL-2-armored pMHC IgG modality referred to herein as guided pMHC staging (GPS). The GPS modality is a bispecific immune engager incorporating a pMHC class I domain and a TAA-targeting domain as the active arms. As proof-of-concept (POC), we focused on redirecting human leukocyte antigen (HLA)-A*02:01 CMV-specific antiviral effector memory T cells given that CMV is a persistent and ubiquitous infection in which prevalence increases with age.[24–28] Greater than 60% of adults over the age of 50 are estimated to be CMV seropositive worldwide.[28] Here we show that IL-2-armored GPS promotes robust expansion of CMVpp65 CD8+ effector memory T cells and induces potent cytotoxic activity against target cancer cells. Comparable to GPS, IL-2-armored GPS significantly reduces CD4+ T cell activation and pro-inflammatory cytokine release relative to a control anti-CD3 TCE. *In vivo* IL-2-armored GPS expands grafted CMVpp65 CD8+ T cells from unstimulated human PBMCs in NSG mice. The IL-2-armored GPS modality also shows favorable developability and monoclonal antibody (mAb)-like PK. Overall, IL-2-armored GPS may represent an attractive general therapeutic strategy for the selective expansion and re-direction of antiviral T cells to eliminate cancer cells with favorable cytokine release.

Results

Design, production and characterization of GPS

To generate POC GPS constructs, we utilized the DuetMab molecule, which incorporates knob-into-hole engineering for hetero Fc pairing and has been widely used as a framework for clinical-stage biologics, as a scaffold.[29–34] We used an epidermal growth factor receptor (EGFR) binding moiety as the TAA-targeting domain and a CMV-specific nonameric peptide pp65$_{495-503}$ (pp65) presented in the context of HLA-A*02:01 as the pMHC domain (Figure 2a, Supplementary Figure S1). In terms of molecular design, clone GA201 was selected as the anti-EGFR targeting antigen-binding fragment (Fab),[35] which was incorporated N-terminally to the hole-side IgG1 Fc region. The

HLA-A*02:01 allele was selected for the pMHC domain, based on its high frequency globally[36–38] and was incorporated N-terminally to the knob-side IgG1 Fc region as summarized in Supplementary Figure S1. The pMHC moiety was engineered as a single-chain pMHC fusion protein such that the peptide was anchored to the HLA groove via a "disulfide trap" as previously reported.[17] The Fc regions were designed with mutations to abrogate the binding of Fcγ receptors.

For production of GPS molecules, constructs were expressed via transient transfection in CHO-K1 cells and purified via protein A affinity chromatography, followed by polishing to a purity of greater than 95% monomer via size exclusion chromatography. The constructs were validated for low endotoxin (below 1 EU/mg) and further interrogated by liquid chromatography-mass spectrometry (LC-MS) to validate the intact and digested molecular masses. As shown in Supplementary Figure S2, the LC-MS spectra for GPS revealed expected molecular masses, consistent with those calculated from the amino acid sequences.

GPS shows favorable bioactivity and cytokine release relative to a conventional T cell engager

To evaluate the bioactivity of GPS *in vitro*, we conducted assays for cytotoxicity, T cell activation and cytokine release using a conventional TCE as a benchmark containing the same TAA targeting moiety (anti-EGFR), an anti-CD3 Fab domain (clone UCHT1),[1] and the same DuetMab scaffold (Figure 2a). In terms of assay design, NCI-H358 cancer cells, which endogenously express EGFR, were used as target cells. PBMCs from CMV+, HLA-A*02:01+ donors were expanded with pp65 peptide and soluble, recombinant human IL-2. The expanded cells were subsequently used as effector cells at an effector-to-target cell (E:T) ratio of 10 to 1. As shown in Figure 2b and Supplementary Figure S3, GPS exhibited potent cytotoxic activity and CD8+ T cell activation, which in some donors were superior to that observed for the conventional TCE treatment in terms of EC$_{50}$. Moreover, GPS notably showed distinct T cell activation and cytokine release profiles compared to conventional TCE treatment in that GPS treatment resulted in significantly reduced CD4+ T cell activation (Supplementary Figure S3C) and pro-inflammatory cytokine release, including IL-6, tumor necrosis factor (Figure 2c,d) and interferon-γ (Supplementary Figure S4). Altogether, these data demonstrate that GPS shows significantly broadened TI relative to conventional TCE treatment.

GPS exhibits limited cytotoxic activity in the context of non-expanded PBMC effector cells

Based on the observed potent cytotoxic activity and improved TI for GPS relative to TCE treatment in the context of pre-expanded PBMCs, we sought to evaluate GPS cytotoxicity in the context of non-expanded PBMC effector cells from the same CMV+, HLA-A*02:01+ donors. As shown in Supplementary Figure S5A, B, GPS induced minimal cytotoxic activity against NCI-H358 target cells across multiple donors in this setting, whereas conventional TCE treatment largely retained cytotoxic activity. We hypothesize that the limited
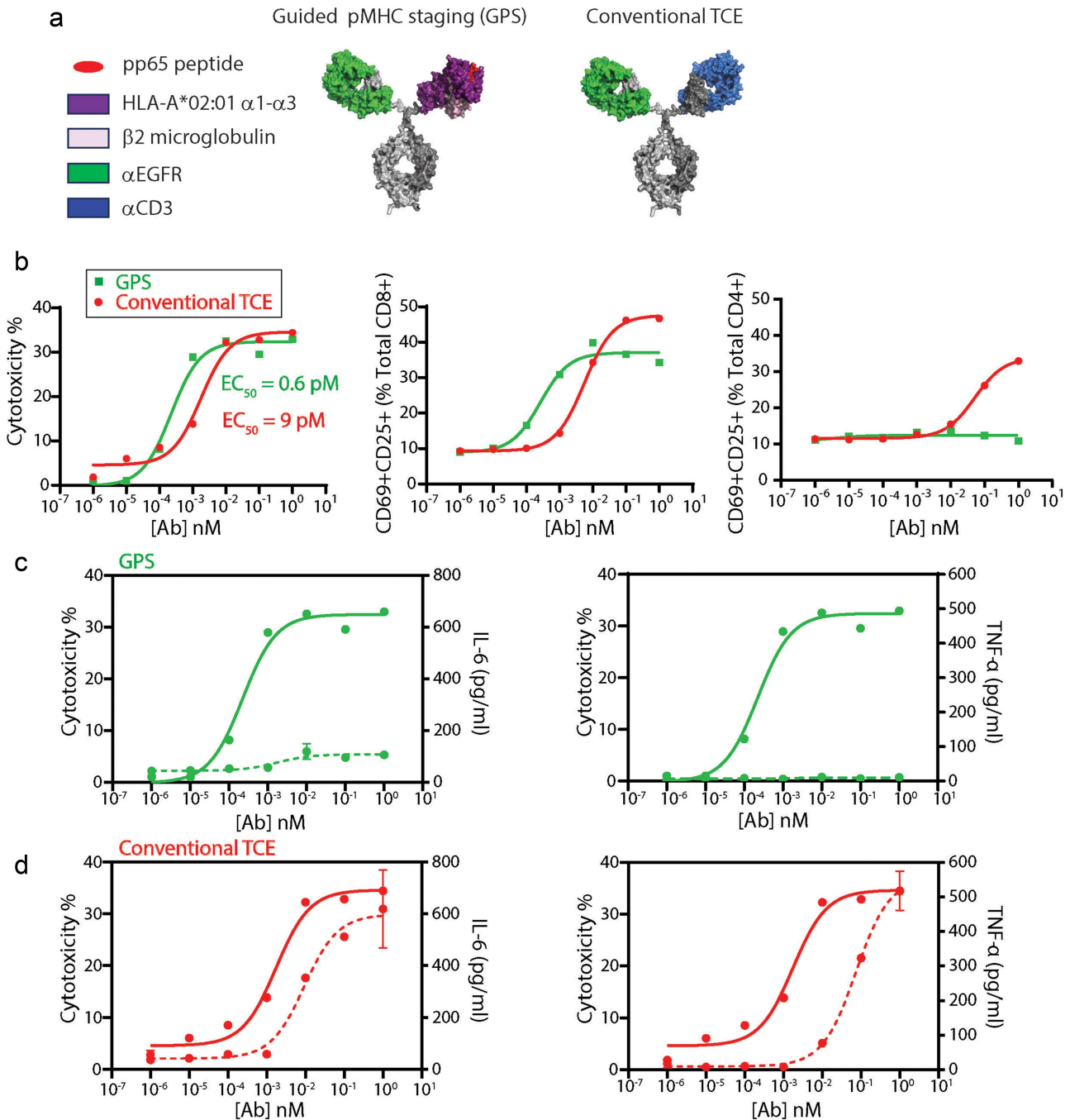
Figure 2. GPS induces potent cytotoxic activity in the context of pre-expanded PBMC effector cells with significantly reduced pro-inflammatory cytokine release relative to a conventional TCE. (a). Schematic depiction of GPS and conventional TCE b-d. GPS (green) or conventional TCE (red) treatment groups were evaluated for the ability to induce cytotoxic activity against NCI-H358 cancer cells using pp65/IL-2 expanded PBMCs as effector cells (b-d). Cytotoxicity, T cell activation and cytokine release (b) were determined 24-hours post treatment. (c-d). Pro-inflammatory cytokine release (dashed lines) is depicted on the right y-axes and % cytotoxicity (solid lines) is shown on the left y-axes for comparison of therapeutic indices. Error bars are SEM. Results shown are representative from one of five independent experiments from five different donors.

cytotoxicity of GPS in these settings is attributed to the low frequency of CMV-reactive cells, given that we routinely observed less than 2% CMV+ cells among viable CD8+ T cells as assessed by tetramer staining. This finding is in contrast to data reported by Schmittnaegel et al., where the authors observed tumor cell lysis in three donors with 3.3%, 1.3% and 0.09% CMV+ cells, respectively.[18] Altogether, these observations highlight the unique effector cell requirements for GPS bioactivity relative to a conventional TCE and suggest

the important role of antiviral T cell expansion for GPS bioactivity, particularly when the initial percentage of CMV-reactive cells within the PBMC population is low.

To corroborate the hypothesis that CMV-reactive antiviral T cells were insufficient to confer cytotoxic activity in the context of non-expanded PBMC effector cells, we evaluated GPS bioactivity against NCI-H358 cells using varying cell numbers of expanded PBMCs and a fixed number of target cells. As shown in Supplementary Figure S5C, D we observed
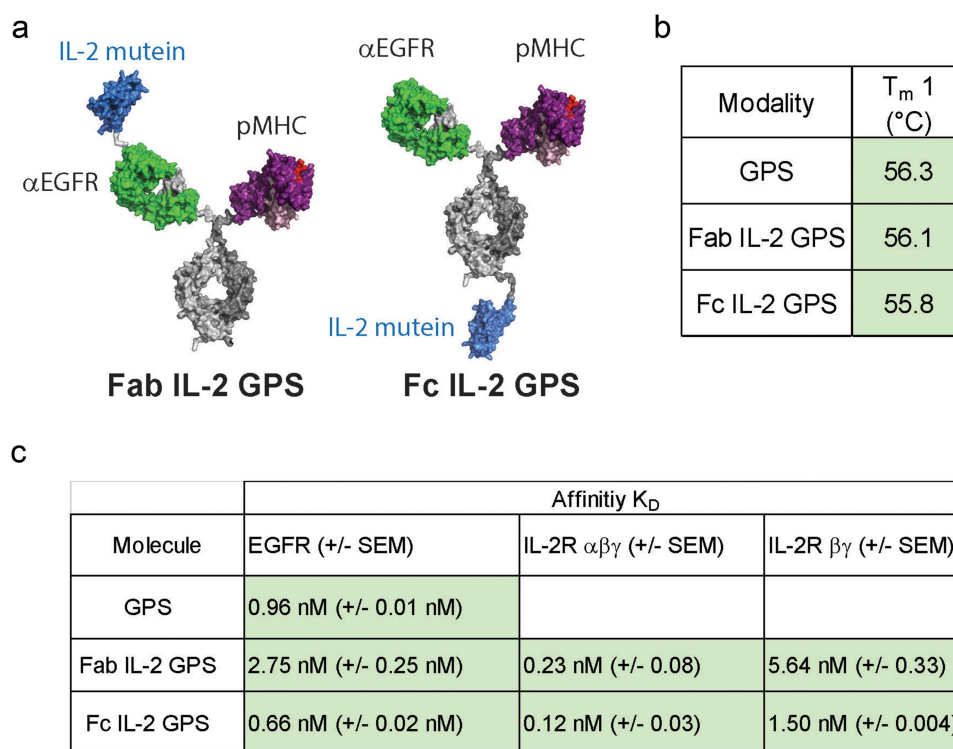
after 48-hour treatment that the degree of cytotoxicity decreased proportionally with the number expanded antiviral effector cells. We further observed that the level of antiviral cells required for partial and complete cytotoxic responses varied in a PBMC donor-dependent manner Supplementary Figure S5C, D. Collectively, these findings strongly suggest the requirement for CMV-specific effector memory cell expansion to achieve potent bioactivity.

GPS and IL-2 GPS modalities exhibit favorable thermal stability and antigen binding

Based on the limited cytotoxic activity of GPS in the context of non-expanded PBMCs, we sought to generate GPS capable of both inducing antiviral T cell expansion and redirecting antiviral cells as TCEs. As shown in Figure 3(a), we engineered IL-2 GPS by covalent fusion of a monovalent IL-2 mutein (H16A, F42A). The H16A, F42A IL-2 mutein was selected based on its reported ~ 100-fold reduced binding to IL-2 receptor (IL-2R)α and ~ 3-fold reduced binding to IL-2 Rβ[39] Relative to wild-type IL-2, the IL-2 mutein was anticipated to improve selectivity for the intermediate-affinity, dimeric IL-2 Rβγ receptor complex expressed on effector T cells by way of attenuated engagement with the high-affinity, trimeric IL-2 Rαβγ complex expressed on Tregs. To understand the impact of IL-2 mutein placement on molecule developability and biological activity, we generated three molecular formats by covalently appending the IL-2 mutein to different locations: 1) N-terminally to the αEGFR Fab (Fab IL-2 GPS), 2) C-terminally to the knob side Fc

(Fc IL-2 GPS), and 3) N-terminally to the pMHC domain (pMHC IL-2 GPS). The IL-2 mutein moiety was flanked by a flexible (G4S)2 linker. We further generated negative controls for GPS and IL-2 GPS molecules by replacing pp65 with the irrelevant peptide [NLTHVLYPV] preferentially expressed antigen in melanoma (PRAME), or by replacing the anti-EGFR domain with the TAA null control Fab (NIP228).

The molecules were produced and evaluated by quality control metrics analogous to those described for GPS lacking IL-2 mutein fusion (Supplementary Figure S6). Notably, IL-2 mutein fusion had limited impact on expression titer and percent monomer relative to GPS for both the Fab IL-2 GPS and Fc IL-2 GPS formats. Significant aggregation was observed for the pMHC IL-2 GPS format, which was therefore discontinued from further assessment. LC-MS spectra of IL-2 GPS molecules indicate masses consistent with glycosylated protein, which is expected for both natural and CHO-expressed IL-2.[40] To further interrogate the molecular masses, deglycosylation treatment was conducted prior to the LC-MS analyses. As shown in Supplementary Figure S6, the LC-MS spectra of Fab IL-2 GPS following deglycosylation revealed intact and reduced masses that were consistent with the calculated masses without glycosylation. LC-MS spectra of the Fc IL-2 GPS and control constructs indicated that N- and O-linked glycosylation were not completely removed by standard deglycosylation treatment. Future investigation outside the scope of this work is warranted to optimize the deglycosylation of these molecules, systematically characterize these glycan species and glycosylation sites, and address glycosylation liabilities relating to product development.

Modality	T_m 1 (°C)
GPS	56.3
Fab IL-2 GPS	56.1
Fc IL-2 GPS	55.8

Molecule	EGFR (+/- SEM)	IL-2R αβγ (+/- SEM)	IL-2R βγ (+/- SEM)
GPS	0.96 nM (+/- 0.01 nM)		
Fab IL-2 GPS	2.75 nM (+/- 0.25 nM)	0.23 nM (+/- 0.08)	5.64 nM (+/- 0.33)
Fc IL-2 GPS	0.66 nM (+/- 0.02 nM)	0.12 nM (+/- 0.03)	1.50 nM (+/- 0.004)

Figure 3. GPS and IL-2 GPS modalities exhibit favorable thermal stability, antigen binding. (a) Schematic depiction of GPS armed with IL-2 mutein fused at either the N-terminus of the hole-side heavy chain (Fab IL-2 GPS) or C-terminus of the knob-side heavy chain (Fc IL-2 GPS) (b) Summary of thermostability (Tm) assessed via DSF (c) Summary of octet binding kinetic analyses. Octet analyses are averages of two independent experiments and error values are SEM.

To assess the developability and translational potential of our GPS platform technology, we characterized GPS and IL-2 GPS molecules for thermal stability and antigen binding. As shown in Figure 3(b), GPS exhibited a melting temperature (T_m) of 56.3°C as assessed by differential scanning fluorimetry (DSF). Further, IL-2 mutein fusion had limited impact on T_m, given that Fab IL-2 GPS and Fc IL-2 GPS had T_m of 56.1°C and 55.8°C, respectively. Overall, both GPS and IL-2 GPS exhibited acceptable thermal stability, significantly above physiological and accelerated storage assessment temperatures.[41]

To characterize TAA binding, we used Octet to characterize GPS and IL-2 GPS binding to the biotinylated EGFR ectodomain using streptavidin biosensors for antigen capture. As summarized in Figure 4(c), kinetic analyses revealed sub-nanomolar αEGFR affinities for GPS ($K_D = 0.96 \pm 0.01$ nM) and Fc IL-2 GPS ($K_D = 0.66 \pm 0.02$ nM), consistent with the reported affinity for clone GA201.[29] Interestingly, Fab IL-2 GPS showed modestly impaired αEGFR affinity ($K_D = 2.75 \pm 0.25$ nM), i.e., approximately 5-fold reduced relative to Fc IL-2 GPS. Altogether, these observations suggest that IL-2 mutein
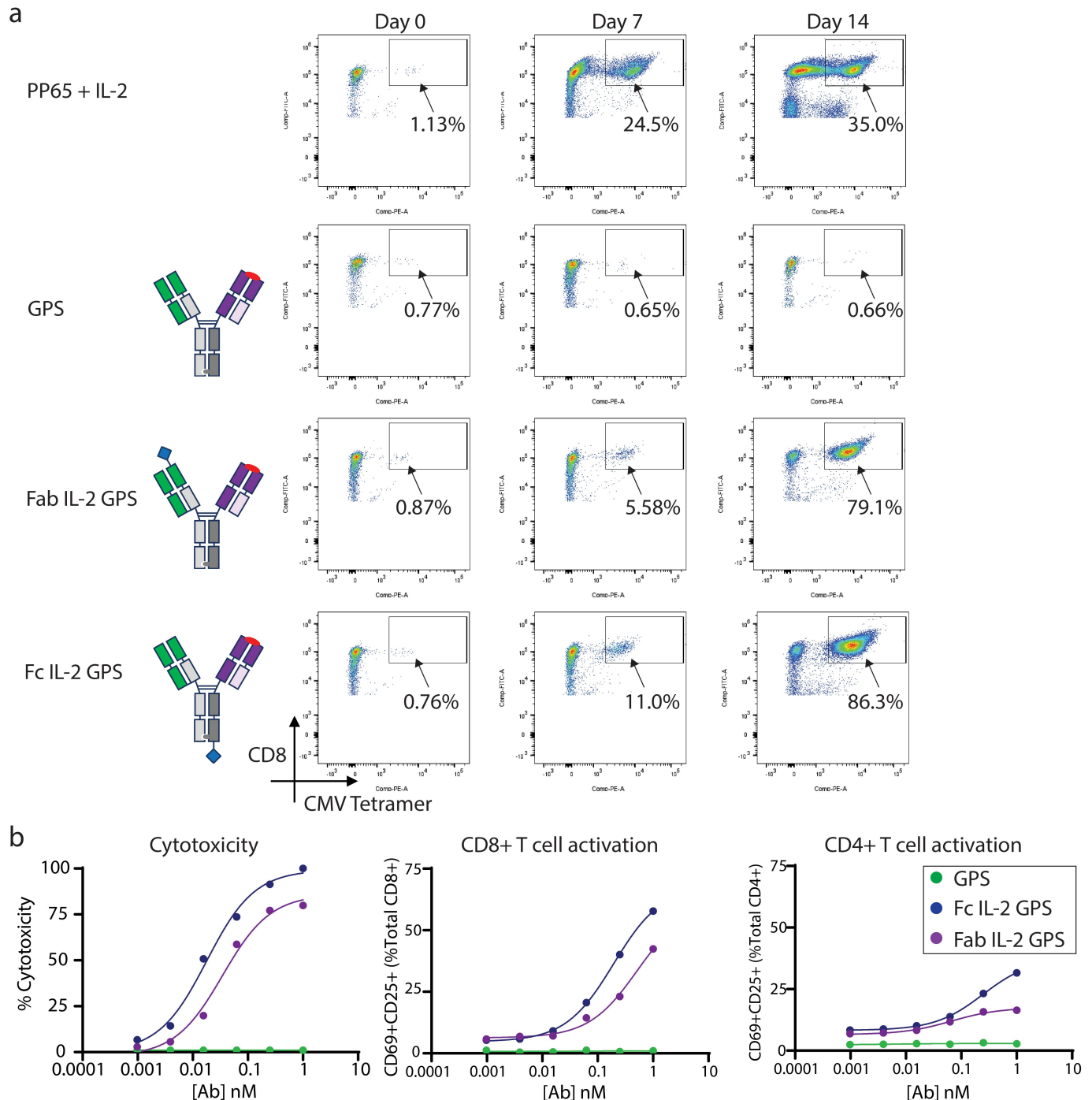
Figure 4. IL-2 GPS promote robust expansion of cmv-specific effector, memory CD8+ T cells. (a) PBMCs were treated with 6 nM test article (GPS, Fab IL-2 GPS, or Fc IL-2 GPS) or positive control (1 ug/mL pp65, 30 units/mL IL-2) in 24 well GREX plates and evaluated for antigen-specific T cell expansion at days 0, 7, and 14 via tetramer staining and flow cytometry. FACS plots are representative from one of four independent experiments with four different donors. (b) Expanded PBMC samples from a were employed as effector cells in cytotoxicity assays against NCI-H358 cells by adding serial-diluted, treatment-group matching test articles. Cytotoxicity and T cell activation was evaluated 48 hours post treatment.

placement proximal to the anti-EGFR Fab partially occludes EGFR binding via steric hindrance.

To characterize IL-2 binding, we employed Octet analyses using the high-affinity IL-2 Rαβγ and intermediate affinity IL-2 Rβγ IL-2 R complexes as antigens. As summarized in Figure 3(c), Fab IL-2 GPS and Fc IL-2 GPS constructs engaged the high-affinity IL-2 R complex with $K_D = 0.23 \pm 0.08$ nM and $K_D = 0.12 \pm 0.03$ nM, respectively, which were significantly impaired relative to the reported wildtype IL-2:IL-2 Rαβγ interaction (K_D of ~0.01 nM).[42] Further, Fab IL-2 GPS and Fc IL-2 GPS showed only modestly impaired binding to the intermediate-affinity IL-2 R complex ($K_D = 5.64 \pm 0.33$ nM and $K_D = 1.5 \pm 0.004$ nM, respectively) compared to the reported wild-type IL-2:IL-2 Rαβγ interaction (K_D of ~1 nM). Altogether, these data demonstrate that the IL-2 R binding properties for the IL-2 GPS constructs are consistent with the reported selectivity of the IL-2 mutein (H16A, F42A).[39] Further, these data indicate that the Fc IL-2 GPS format shows modestly enhanced binding to both high-affinity and intermediate affinity IL-2 R complexes compared to the Fab IL-2 GPS format.

IL-2-armored GPS robustly expands CMV-specific CD8+ effector memory T cells and confers potent cytotoxic activity as a TCE

Building upon the entirety of these findings, we investigated the capacity of IL-2-armored GPS constructs to expand CMV-specific effector memory CD8+ T cells from CMV+, HLA-A*02:01+ PBMCs. In terms of assay design, we treated PBMCs with test articles (6 nM) for 14 days in 24-well G-REX plates and characterized the kinetics of CMV antiviral cell expansion by staining with fluorescently labeled pMHC tetramers (pp65/HLA-A*02:01) at days 0, 3, 7, and 14. As shown in Figure 4(a), limited expansion was observed at day 0 and day 3 timepoints for all test groups. At day 7 and day 14, clear expansion was observed in the positive control group (pp65 + IL-2) with the percentage of CMV+ cells among viable CD8+ T cells reaching 24.5% and 35.0% for days 7 and 14, respectively. At day 7, Fab IL-2 GPS and Fc IL-2 GPS induced modest expansion with 5.5% and 11.0% CMV+ cells among viable CD8+ T cells, respectively. GPS lacking IL-2 mutein fusion showed no evidence of expansion for the same donor at the 7-day time point (Figure 4(a)). By day 14, Fab IL-2 GPS and Fc IL-2 GPS treatment groups both strikingly showed substantial expansion, quantified at 79.1% and 86.3%, respectively. Altogether, IL-2 GPS molecules showed robust capacity to significantly expand CMV-reactive cells in multiple donors (Supplementary Figures S7-S8), beginning at Day 7 and increasing by Day 14, which is in contrast to GPS lacking IL-2 mutein fusion, which conferred limited potential to expand CMV+ cells within 14 days, with only modest expansion observed in a donor-dependent manner.

To test whether the IL-2-armored GPS expanded PBMCs could then be re-directed for subsequent killing as effector cells, we conducted subsequent *in vitro* cytotoxicity assays. The test article-expanded PBMCs were rested, washed and applied directly as effector cells following the 14-day expansion. Serially diluted test articles matching the treatment group

for the expansion were added as treatment. As shown in Figure 4(b) and Supplementary Figure S8C, both Fab IL-2 GPS and Fc IL-2 GPS induced potent cytotoxic activity against NCI-H358 cells, whereas GPS showed limited cytotoxic activity in this assay, consistent with the observed lack of expansion. We observed modest enhancement in cytotoxic activity for Fc IL-2 GPS relative to Fab IL-2 GPS, which corresponded with the observed modest increase in expansion as well as the observed higher relative αEGFR binding affinity. To further assess the relative killing capacity of IL-2-armored GPS compared to GPS lacking IL-2 mutein fusion when the frequency of CMV-specific effector memory cells is high and controlled across groups, we evaluated relative cytotoxic activity in the context of pp65 IL-2 expanded PBMC effector cells. As shown in Supplementary Figure S9, Fc IL-2 GPS and Fab IL-2 GPS exhibited potent cytotoxic activity against NCI-H358 cancer cells in multiple donors, similar to that observed for GPS treatment. Altogether, these data highlight the significance of anti-viral effector memory cell expansion as a requirement for potent GPS bioactivity.

To evaluate the capacity of IL-2 GPS to both expand CMV-specific antiviral T cells in the presence of cancer cells and induce cytotoxic activity in a 'one-pot assay', we used Fab IL-2 GPS and control constructs of the same format (*i.e.*, incorporating the TAA-null NIP228 Fab or the CMV peptide-null PRAME pMHC) as POC test articles. The goal was to understand the influence of each active domain (*i.e.*, anti-EGFR, pMHC and IL-2 mutein) on antiviral T cell expansion and anti-cancer cytotoxic activity (Figure 5(a)). In terms of assay design, NCI-H358 cells (5e3 cells per well) were seeded in 96-well plates and then 24-hours post seeding, non-expanded PBMCs and test articles were added to the wells. Cell growth was monitored by xCELLigence over 14 days and tetramer staining was conducted at the end point. As shown in Figure 5(b), only the Fab IL-2 GPS and Fab IL-2 GPS NIP228 treatment groups induced significant expansion at day 14, indicating that active domains for both pMHC and IL-2 are required for CMV+ antiviral T cell expansion. As shown in Figure 5(c), Fab IL-2 GPS exhibited higher cytotoxic activity relative to control treatment groups. Overall, these data indicate that all three functional domains (*i.e.*, anti-EGFR, pMHC and IL-2) are needed for optimal cytotoxic activity.

IL-2-armored GPS selectively expands CMVpp65-specific CD8+ T cells

To evaluate the selectivity of IL-2-armored GPS-mediated CMVpp65-specific CD8+ T cell expansion, whole PBMCs from HLA-A*02:01+healthy CMV+ donors were cultured in the presence of GPS, IL-2-armored GPS, or control and the frequency of immune cell subsets (CMVpp65-specific, nonspecific CD8+ T cells, natural killer (NK) cells, Tregs and conventional CD4+ T cells) were evaluated after 11 days by flow cytometry. As shown in Figure 6(a), IL-2-armored GPS expanded CMVpp65-specific CD8+ T cells in a concentration dependent manner. As expected, neither GPS nor IL-2-armored PRAME GPS molecules expanded CMVpp65-specific CD8+ T cells. As shown in Figure 6(b), CMVpp65 IL-2-armored GPS molecules also induced expansion
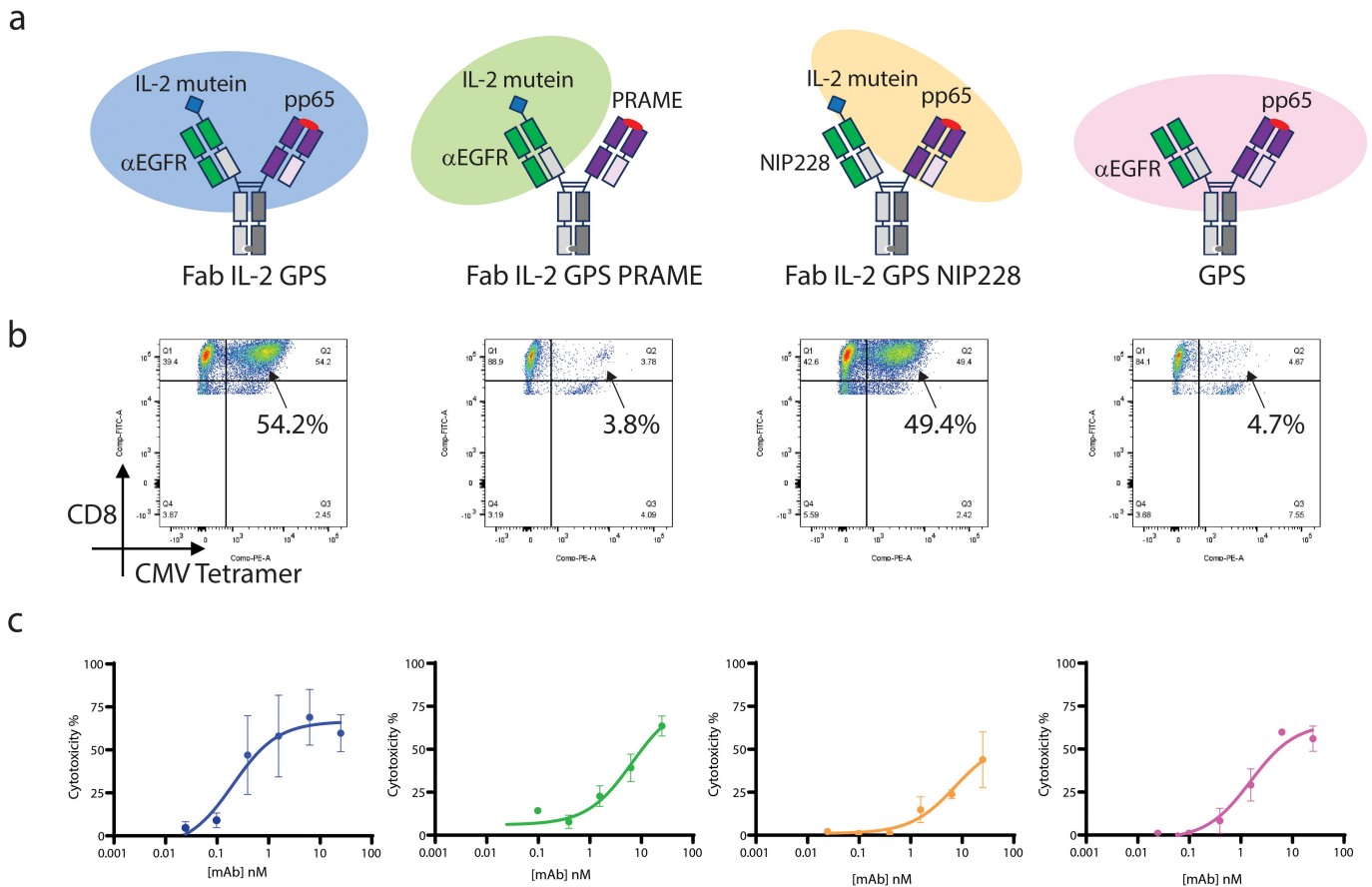
Figure 5. IL-2 GPS expand CMV-specific effector, memory CD8+ T cells in the presence of NCI-H358 cells leading to potent tumor cell killing (a) Schematic depiction of Fab IL-2 GPS, irrelevant pMHC control (Fab IL-2 GPS PRAME), TAA control (Fab IL-2 GPS NIP228), and GPS. The active molecular domains are highlighted in blue, green, yellow and pink, respectively. (b and c) Test articles were evaluated in the one-pot expansion and killing assay using non-expanded PBMCs as effector cells. (b) Following 14 days of treatment, CMV+ antiviral cell expansion was assessed by tetramer staining as shown for the 6.25 nM treatment group. (c) % cytotoxicity was determined by xCelligence as shown at the 14 day post-treatment condition. Error bars are SEM ($n = 2$). Expansion and cytotoxicity data correspond with the test article in each of the four columns, with cytotoxicity curve fits colored as blue (Fab IL-2 GPS), green (Fab IL-2 GPS PRAME), orange (Fab IL-2 GPS NIP228), and pink (GPS), respectively. Data shown are representative from one of three independent experiments.

of other immune cell subsets including NK cells and to a lesser extent CD4 Tregs compared to the observed expansion of CMVpp65-specific CD8+ T cells. These observations may be attributed to expression of IL-2 Rβγ on NK cells and IL-2 Rαβγ on Tregs, respectively.[43] In line with these observations, NK cell expansion has also been reported for the clinical-stage pMHC IgG CUE-101, which likewise contains the IL-2 mutein F42A, H16A.[39] To improve the selectivity for virus-reactive effector memory cells, further optimization of the IL-2 mutein fusion moiety may be warranted such as by engineering conditionality to 'turn on' IL-2 mutein binding activity only upon GPS engagement with cognate T cell receptors (TCRs), or alternatively by further modulating IL-2 mutein specificity by, for example, further reducing affinity to IL-2Rα. In order to further probe the expansion specificity, we evaluated the frequency of circulating human T cell subsets (*i.e.*, naïve, central memory (TCM), effector memory (TEM), and terminal effector (TEMRA)) among CMVpp65-specific CD8+ and non-CMVpp65-specific CD8+ T cells following test article treatment of the PBMCs for 11 days. As shown in Supplementary Figure S10, IL-2-armored GPS molecules mediated the expansion of pp65 CD8+ TEM cells in an antigen-specific manner. The lack of pp65 CD8+

TEM expansion with IL-2-armored PRAME GPS treatment and lack of non-CMV CD8+ TEM expansion with IL-2-armored GPS treatments further corroborates the selective nature of these molecules in expanding and maintaining the CMV-specific CD8+ TEM cells.

GPS and IL-2-armored GPS exhibit mAb-like PK in vivo

To model the PK properties of GPS and IL-2 GPS *in vivo*, Tg32 transgenic mice expressing human neonatal Fc receptor (FcRn) were injected with a single intravenous dose (5 mg/kg) of GPS, Fab IL-2 GPS, or Fc IL-2 GPS. Sera samples were collected across 6-time points spanning 35 days and human IgG content was determined by ELISA. As shown in Figure 7, GPS and IL-2 GPS constructs remained detectable in sera samples throughout the 35-day period at levels higher than those required for *in vitro* bioactivity. Altogether, these data suggest acceptable PK for the GPS modalities. Future investigation is warranted to further characterize PK in terms of half-life and clearance rate, especially using *in vivo* models possessing human IL-2Rs that may impact PK properties.
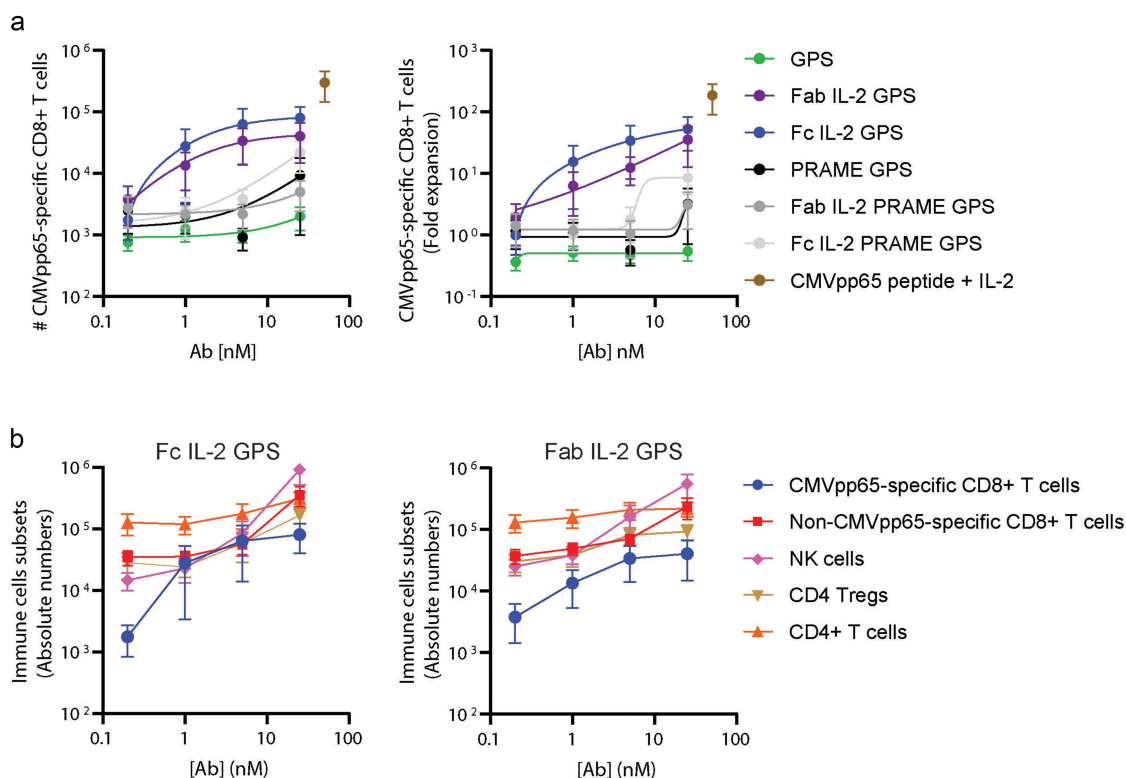
Figure 6. IL-2-armored GPS molecules selectively expand CMVpp65-specific CD8+ T cells. Whole PBMCs from HLA-A*02:01+ healthy CMV+ donors were cultured in the presence of various concentrations of GPS molecules for a period of 10-11 days for a period of 10-11 days. (a) The absolute number and fold expansion (mean ± SEM) of CMVpp65-specific CD8+ T cells on day 10-11 of culture with GPS and IL-2-armored GPS molecules. As a positive control, PBMCs were stimulated with CMVpp65 peptide + wildtype IL-2. Data shown here are from six individual donors from two independent experiments. (b) The absolute number (mean± SEM) of CMVpp65-specific and nonspecific CD8+ T cells, NK cells, CD4 tregs and total CD4+ T cells on day 10-11 of PBMC culture with Fc IL-2 GPS or Fab IL-2 GPS molecules. Data shown are from six individual donors from two independent experiments.
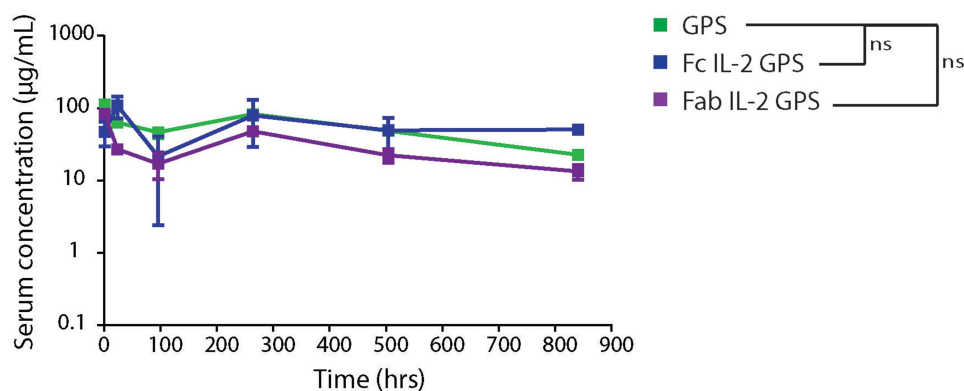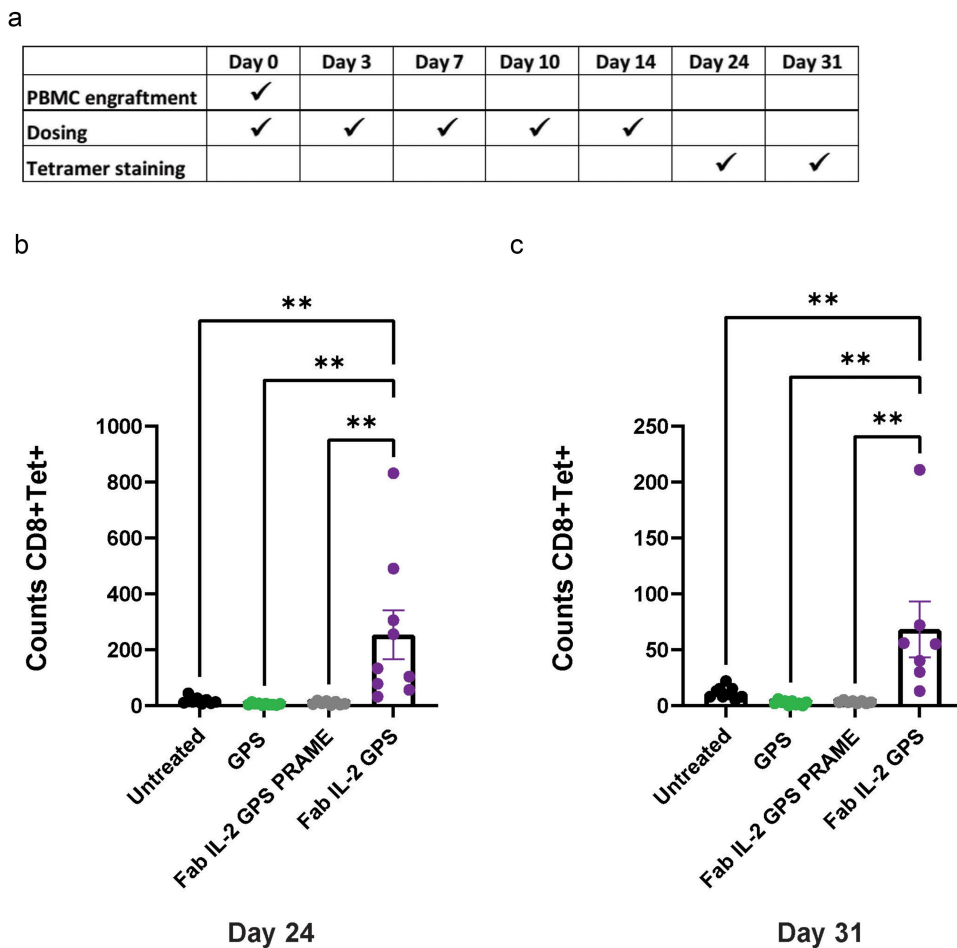

Figure 7. GPS and IL-2 GPS modalities exhibit mAb-like pharmacokinetics in Tg32 mice. PK analysis of GPS, Fab IL-2 GPS and Fc IL-2 GPS administered via a single intravenous dose of 5 mg/kg in female Tg32 mice ($n = 3$ per group) with human IgG serum content determined by ELISA. The error bars are SEM. 'ns' refers to no significant difference for the area under the curve based on one-way ANOVA with Tukey multiple comparisons test.

IL-2-armored GPS expands CMV reactive CD8+ memory cells *in vivo*

To examine whether the IL-2-armored GPS was capable of expanding CMV-specific memory cells *in vivo*, we adoptively transferred 2e6 unstimulated PMBCs from one of our HLA-A*02:01 CMV+ positive donors into a NSG host. The untreated group instead received adoptive transfer of pre-expanded PBMCs from a HLA-A*02:01+, CMV+ positive donor (2e6 per mouse). The animals were dosed at 1 mg/kg with Fab IL-2 GPS, PRAME IL-2 GPS and GPS for a total of five doses, on days 0, 3, 7, 10, and

14. Blood was drawn and subsequently stained for CMV+ CD8+ cells on day 24 and day 31. As shown in Figure 8 and Supplementary Figure S11, of the three test articles, only Fab IL-2 GPS demonstrated significant expansion of tetramer positive CD8+ memory cells. In the GPS animals and untreated animals, limited viable adoptive T cells were observed after 24 days, suggesting the potential need for IL-2 stimulation or additional molecular cues to maintain T cell viability in this setting. Altogether, these data notably establish POC that IL-2-armored GPS expands CMV-specific effector memory cells *in vivo*.

a

	Day 0	Day 3	Day 7	Day 10	Day 14	Day 24	Day 31
PBMC engraftment	✓						
Dosing	✓	✓	✓	✓	✓		
Tetramer staining						✓	✓

Figure 8. IL-2-armored GPS expands CMV-reactive effector, memory CD8+ T cells *in vivo*. (a) Summary of in vivo assay design: female NSG mice (NOD.Cg-Prkdc[scid]IL-2Rg[tm1Wjl]/SzJ) aged 6 to 8 weeks (*n* = 10 per group) received adoptive transfer of unstimulated PBMCs from a HLA-A*02:01+, CMV+ donor (2e6 per mouse) on day 0. Mice were dosed with Fab IL-2 GPS, Fab IL-2 GPS PRAME and GPS (1 mg/kg) on days 0, 3, 7, 10, and 14. On day 24 (b) and day 31 (c), blood samples were collected and analyzed for expansion via tetramer staining and flow cytometry analysis. The untreated group received adoptive transfer of pre-expanded PBMCs from a HLA-A*02:01 +, CMV+ donor (2e6 per mouse) on day 0. For statistical analyses, ** indicates $p < 0.0021$ as assessed by Tukey multiple comparison test. Error bars are SEM. Outliers were calculated and removed using the ROUT method with Q set to 1%.

Discussion

In this study, we report on the IL-2-armored GPS as an optimized pMHC bispecific TCE modality for potential therapeutic applications against hematological and solid malignancies. We find that IL-2-armored GPS is well-suited to overcome the safety limitations of existing TCE strategies while maintaining potent cytotoxicity, even when the frequency of anti-viral cells in circulation is low. We demonstrate *in vitro* that IL-2-armored GPS significantly enhances anti-cancer activity in the context of non-expanded PBMC effector cells. To our knowledge, IL-2-armored GPS is the first reported pMHC modality that both robustly expands and specifically redirects CD8+ virus-specific effector memory cells.[12,17,19–21,39,44,45] We present a focused POC evaluation of IL-2-armored GPS for the redirection of CMV-reactive effector memory cells. In our internal investigations, we are actively exploring the engineering and redirection of a wide range of antiviral cells, covering additional HLA types as well as different virus-specific peptides, e.g., SARS-CoV-2, EBV, influenza. Overall, we anticipate that the GPS platform technology may be broadly applied for the expansion and redirection of immune cells for the treatment of cancer and other pathologies.

Several engineered IgGs containing pMHC and cytokines domains, *i.e.*, non-native IgG components, have advanced to clinical trials. Such molecules, which are distinct from GPS and other pMHC IgGs[17–19] in that they lack an TAA-targeting arm, highlight the general translational potential of pMHC modalities. The most clinically advanced pMHC fusion protein is CUE-101, which is undergoing evaluation in a Phase 1 clinical trial (NCT03978689) for the treatment of human papillomavirus (HPV)-positive head and neck squamous cell carcinoma as either a monotherapy or in combination with PD-1 inhibitory pembrolizumab (Keytruda®).[39,44] In terms of molecular design, CUE-101 is an Fc fusion protein containing two pMHC domains (HPV16 E7$_{11-20}$ – HLA-A*02:01) and four IL-2 mutein domains, designed to respectively deliver primary activation signal and cytokine support for the expansion of CD8+ tumor-specific memory T cells. Several additional pMHC fusion proteins aimed at expanding tumor-specific memory CD8+ T cells are in clinical development, including CUE-102 (NCT05360680), which expands Wilms' Tumor 1 (WT1) tumor-specific memory CD8+ T cells for the treatment of various cancer indications. Overall, progress on the clinical

development of pMHC fusion proteins motivates the continued development of next-generation modalities, especially those possessing unique mechanisms of biological activity.

One clear distinction between the clinical development-stage pMHC modalities (*i.e.*, CUE-101 and CUE-102) and IL-2-armored GPS relates to their respective 'passive' versus 'active' mechanisms of action in terms of cytotoxic activity. The former relies on antigen-specific cytotoxic lymphocytes to recognize endogenous pMHC on the cancer cell surface, whereas GPS actively recruits cytotoxic lymphocytes to synapse with cancer cells, thereby inducing cytotoxic activity as a TAA-targeted TCE. As a result, current clinical-trial stage pMHC therapeutics may be limited by evasion and resistance mechanisms owing to HLA mutations and downregulation, HLA loss of heterozygosity and β2M loss, as has also been observed for various immuno-oncology (IO) therapies.[46–53] By contrast, GPS can potentially overcome these evasion and resistance mechanisms. In particular, GPS may show utility in tumor settings characterized by a low frequency of neoantigens in which IO therapy is less efficacious due to the ability to redirect highly reactive viral-specific cytotoxic lymphocytes.

Beyond the approach of IL-2 mediated T cell expansion, recent preclinical research showcases alternative approaches to achieving antiviral cell expansion.[19,45] For example, Li et al. demonstrate the utility of multivalent pMHC biologics armed with co-stimulatory domains targeting CD28 and CD137 for the selective expansion of CMV or HIV antiviral cells for the application of inhibiting viral infection.[45] By extension, GPS could foreseeably be engineered with alternative molecular cues to modulate the expansion of antiviral cells and potentially modulate other properties relating to biologic potency, PK, and pharmacodynamics. In a separate study, Fischer et al. reported on pre-vaccination as an innovative approach to augment bioactivity in the context of murine models.[19] The authors generated and evaluated a bispecific TCE containing two anti-TAA Fab domains that bind to fibroblast activation protein alpha (expressed in 90% of human carcinomas) and a murine-derived MHC arm presenting a murine CMV peptide.[19] They observed that pre-vaccination followed by IgG treatment eliminated tumor growth in some of the *in vivo* cancer models tested, albeit not all, with efficacy correlating with initial tumor size. Overall, the IL-2-armored GPS single molecule approach is unique from the previously reported vaccination strategy and may be desirable in terms of driving local expansion of anti-viral effector, memory cells within the tumor microenvironment.

Previous research on pMHC TCEs both externally and internally has served an important role in informing the development of IL-2-armored GPS.[17–21] In particular, Schmittnaegel et al. evaluated the impact of pMHC valency, TAA valency, and molecular format on bioactivity, safety, and developability to inform the identification of optimized pMHC IgG formats.[17,18] In our internal *in vitro* investigations, GPS containing two pMHC domains showed significantly enhanced potency relative to GPS containing one pMHC domain in cytotoxicity assays using pre-expanded effector cells. Likewise, GPS containing two pMHC domains induced CMV-reactive effector memory cell expansion to some extent in CMV+, HLA-A*02:01+ PBMC donors

samples within 14 days (unpublished data). Others have showcased the favorable attributes of a fusion protein therapy containing an anti-TAA Fab against epithelial cellular adhesion molecule (EpCAM) covalently linked to a pMHC domain presenting pp65 peptide in the context of HLA-B*07:02, which exhibited potent cytotoxic activity and significantly reduced cytokine release relative to the TCE benchmark solitomab, which is an EpCAM/CD3 bispecific TCE.[20] We investigated the cytokine release profile of IL-2-armored GPS treatment relative to GPS lacking IL-2 mutein fusion and observed that IL-2-armored GPS retains an attractive cytokine release profile similar to GPS. Altogether, these findings and others[18] collectively suggest the generality of our observations on the attractive safety profile of the GPS modality relative to conventional TCE treatment.

One potential strategy to further improve GPS cytotoxic potency is modulating the inherent weak interaction between MHC class I and CD8, which is reported as ~140 μM.[54] We generated CD8 affinity-enhanced GPS containing the mutation Q115E in the heavy chain α2 domain, which is reported to enhance CD8:MHC class I to a K_D of 98 μM,[54] and evaluated *in vitro* cytotoxicity using pre-expanded PBMCs from CMV+, HLA-A*02:01+ seropositive donors as effector cells and NCI-H358 target cells. As shown in Supplementary Figure S12, we observed modestly enhanced killing with CD8 affinity-enhanced GPS relative to GPS bearing the wild-type α2 domain. We posit that anti-CD8 affinity-enhanced GPS may augment the recruitment of additional CMV-specific T cells with lower affinity TCRs and may therefore be valuable toward improving TI, particularly for donors that possess antiviral cells with lower affinity TCRs. Overall, future investigation may be warranted to optimize the parameter of anti-CD8 affinity to enhance cytotoxic potency without compromising specificity, cytokine release, and developability.

Further investigation is also warranted to better predict if and under which clinical settings GPS may confer sufficient anti-cancer activity. More comprehensive characterization of the frequency and memory status of anti-viral effector-memory T cells within TMEs may aid in this prediction. Previously, investigators suggested that a pMHC IgG TCE (with bivalent TAA targeting) may be sufficient to potently kill tumor cells, even at low frequency of effector memory cells (*e.g.*, below 1% among CD8+ T cells), which to our knowledge has not been shown *in vivo*.[12] Herein, we suggest that IL-2-armored GPS, or alternative GPS armored with other co-stimulatory molecular cues, may be required to confer anti-cancer activity, particularly if the TME-resident CMV effector memory cell population is low. This is based on the unique mechanism of IL-2 GPS to both expand antiviral T cells and redirect them to synapse with cancer cells. Notably, we identified that all three functional domains of IL-2 GPS are important for mediating anti-cancer activity in terms of cytotoxic activity in the context of non-expanded PBMCs. Previous research indicates that both the expansion of antiviral cells within the tumor microenvironment and the decoration of the cancer cell surface with IL-2[55,56] have the potential to confer intrinsic anti-cancer activity to some extent. Our findings align with these observations, while further illustrating that IL-2 GPS confers anti-tumor activity beyond these mechanisms.

Future investigation is also warranted to comprehensively evaluate the *in vivo* bioactivity of IL-2-armored GPS in terms of efficacy in human xenograft models. Selection of animal host, tumor model, and other assay design parameters likely influence the suitability of *in vivo* efficacy studies. Schmittnaegel et al. have previously shown *in vivo* efficacy of pMHC IgGs against MDA-MB435 tumors in the context of pre-expanded CMV-specific effector memory cells mixed with non-expanded PBMCs in NOG immunodeficient mice.[18] We utilized an NSG mouse model to establish that IL-2-armored GPS treatment expands CMV-specific effector memory cells in the absence of tumor xenograft. While NOG and NSG mice were both developed by backcrossing of IL-2 Rγ^{null} mice, these models are different in that NOG mice produce IL-2Rγ protein that can bind cytokine but not signal, whereas NSG mice do not produce IL-2Rγ.[57] As such, NOG mice may complicate the *in vivo* evaluation of IL-2-armored GPS due to potential sink effects for the IL-2 domain. Mouse surrogate pMHC IgGs have also been successfully used to establish *in vivo* efficacy in mouse tumor models and therefore may be useful for the future investigation of surrogate IL-2-armored GPS molecules.[19] Overall, additional pivotal biological evaluation of the IL-2-armored GPS remains to be conducted in future work to better understand the translational potential of this strategy for the treatment of cancer. Beyond the evaluation of tumor growth inhibition *in vivo*, these studies foreseeably include evaluating: 1) the impact of the IL-2 mutein fusion on the expansion of cell subsets other than CMV-specific memory T cells *in vivo* in the NSG mouse setting, 2) the impact of the IL-2 moiety on cytokine release *in vivo*, 3) the risk of IL-2 armored GPS treatment on immunogenicity, and 4) the pharmacodynamics of anti-viral effector memory cell expansion within the TME and in peripheral tissues.

Comprehensive profiling of anti-viral cell phenotype warrants further discussion and may serve predictive value in identifying CMV+, HLA-A*02:01+ patient populations that are most likely to respond to pMHC IgG therapies. Of the four reported circulating human T cell subsets as defined by their CD45RA, CCR7 expression profile, *i.e.*, naïve, TCM, TEM, and terminal effector TEMRA, persistent CMV-specific CD8+ T cells are largely characterized by TEM and TEMRA phenotypes.[58] The benefit of exploiting and re-directing CMV anti-viral cells owing to this unique late-differentiated TEM and TEMRA memory phenotype (CD45RA- or +, CCR7+, CD62L-, CD27-, and CD28-) is characterized by: 1) the capacity for rapid effector function, 2) resistance to exhaustion, senescence, or dysfunction, 3) enhanced longevity as indicated upregulation of CD127, 4) rapid replenishment, 5) lack of requirement for co-stimulation, and 6) migration to inflamed tissue via expression of CXCR3.[18,58–65]

A patient's CMV-reactive TCR repertoire is also likely to influence responsiveness to pMHC IgG therapies and future investigation is warranted toward characterizing potential determinants, *e.g.*, diversity and frequency of high-affinity TCRs. We profiled the TCRβ CDR3 repertoires for six CMV +, HLA-A*02:01+, CMV tetramer+ PBMC samples after expansion with pp65 and IL-2 treatment by next-generation sequencing (NGS). As shown in Supplementary Table S1, we observed substantial diversity of the TCRβ CDR3 repertoire in terms of unique sequence reads, which aligns with previous reports profiling CMV TCR repertoire diversity.[66] Frequent TCRβ CDR3 sequences were also observed publicly (*i.e.*, across multiple donors) and, importantly, these consensus sequences were corroborated as either identical or highly similar to published CMV-reactive TCRβ CDR3 sequences[66,67] as shown in Supplementary Figure S13. Future investigation comparing the CMV-reactive TCR repertoire for control treatment (expanded via pp65/IL-2) versus IL-2 GPS treatment may also be valuable toward understanding potential mechanistic differences in CMV-reactive T cell expansion.

To our knowledge, CD8-biased TCE modalities have yet to be trialed clinically. GPS represents a specialized CD8-biased modality, designed to engage with a specific subset of CD8+ T cells, while minimizing CD4+ T cell activation and cytokine release. Further investigation is warranted toward interrogating the influence of CD8 bias on TCE bioactivity in preclinical models. One additional consideration would be the potential need for balancing CD8+ and CD4+ T cell activation/redirection as evidenced by the reported role of CD4+ T cells as direct and indirect mediators of anti-cancer activity.[68,69] Overall, our work herein demonstrates the promise of the IL-2-armored GPS as next-generation TCEs for broad therapeutic and anti-cancer applications.

Materials and methods

Tumor cell lines

NCI-H358 (ATCC) and were maintained in RPMI 1640 medium (Gibco) with 10% heat-inactivated fetal bovine serum (HI-FBS, Gibco) and 1% penicillin/streptomycin (P/S). The cells were cultured at 37°C and 5% CO2.

PBMC isolation

PBMCs were isolated from the fresh leukopaks of healthy donors following the manufacturer's protocol (StemCell Technologies, Document #PR00002). PBMCs aliquots were then frozen in CryStor CS10 cryopreservation medium (StemCell Technologies) following the manufacturer's protocol.

Molecule expression, purification and quality control

CHO-K1 cells were transiently transfected with plasmids encoding heavy and light chain sequences at a 1:1 ratio using polyethyleneimine as the transfection reagent. Cellular supernatants were harvested ~14 days post-transfection, sterile filtered, captured via MabSelect SuRe columns (GE Healthcare) and buffer exchanged to phosphate-buffered saline (PBS; pH 7.2). If monomer content was below 95%, the antibodies were further purified via Superdex 200 16/600 column (GE Healthcare) after concentrating samples via Amicon Ultra-15 Centrifugal Filter Units with 50kD NMWL (Millipore Sigma). The percent monomer, and endotoxin level of each purified antibody was determined by analytical size-exclusion chromatography and Endosafe LAL testing (Charles River) to ensure > 95% monomer content and < 1 EU/mg endotoxin.

LC-MS

All analyses were performed on an Agilent 1260 infinity HPLC coupled to an Agilent 6520 Accurate-Mass Q-TOF LC/MS with an electrospray ionization source. The following LC conditions were used: flow rate 0.5 mL/min, mobile phase A contained water with 0.1% formic acid (LC-MS grade) and mobile phase B contained acetonitrile with 0.1% formic acid (LC-MS grade). The step elution condition was as follows: 10% B for 5 min; 90% B for 6 min; 10% B for 3 min. For sample preparation, samples were treated with deglycosylation mix II (NEB) at 37°C for 16 hours. Reduced samples were obtained by treated with 10 mM DTT at 37°C for 30 min. 8 ug of intact antibody, while 2 ug of reduced antibody, were loaded onto a Poroshell 300SB-C3 column (2.1×75 mm, Agilent), MS spectra were acquired over 1000–3000 m/z range, then processed using Agilent Mass Hunter software from Agilent Technologies.

Melting temperature assessment

Protein melting temperatures (T_m and T_{onset}) were determined by DSF using a previously established method with minor modifications.[70] DSF samples were prepared by combining 5 μL of SYPRO Orange dye (diluted with PBS (pH 7.2) to 40X concentration; Invitrogen S-6651) with 20 μL of protein sample at 1 mg/mL in PBS (pH 7.2) in duplicate in a 96-well MicroAmp Optical plate (ThermoFisher N8010560). The plate was sealed and measurements performed in a QuantStudio 7 Flex Real-Time PCR System (Applied Biosystems). Samples were subjected to an initial equilibration step at 25°C for 2 min, followed by a temperature ramp to 99°C at 0.05 °C/sec increments. The fluorescence emission was monitored using the FAM filter set. The T_m value for each sample was calculated in the Protein Thermal Shift software (Applied Biosystems) using the Boltzmann method, and T_{onset} values were approximated from these curves.

Octet binding assessment

Bio-layer interferometry was conducted using the Octet384 instrument (ForteBio) with Octet buffer (PBS, pH 7.2 containing 3 mg/ml bovine serum albumin, and 0.05% Tween-20) as the assay diluent. Biotinylated antigen (2 μg/mL) was loaded onto streptavidin biosensors (Sartorius, catalog #18-5019) and the following antigens were used: biotinylated human EGFR ectodomain (Acro Biosystems, Catalog #: EGR-H82E3), biotinylated IL-2 Rαβγ ectodomain (Acro Biosystems, Catalog #: ILG-H82W9), biotinylated IL-2 Rαβγ ectodomain Fc (Acro Biosystems, Catalog #: ILG-H82F3). In terms of the kinetic binding assay workflow, streptavidin biosensors were first equilibrated in Octet buffer for 10 minutes, and then sequentially dipped into a series of 384-well plate (Sartorius, Catalog #: 18–5076) wells containing: 1) Octet buffer as the sensor check step, 2) biotinylated antigen (2 μg/mL) as the loading step, loaded to 0.5 nanometers, 3) Octet buffer as the equilibration step, 4) serially diluted antibodies as the association step, and 5) Octet buffer as the dissociation step. Data analysis was conducted using Octet 384 software (v.7.2) using a global fit with a 1:1 binding model.

Bioactivity assays

The expansion assays for monitoring the CMV-specific effector, memory CD8+ T cell population were carried out in 6-well and 24-well G-REX plates (Wilson-Wolf). Briefly, PBMCs at a final density of 2e6 cells/mL were treated with antibody, or positive/negative control, diluted into in RPMI 1640 media supplemented with 10% HI-FBS and 1% P/S. The cells were cultured at 37°C and 5% CO2 for 14 days. For positive control treatment, PBMCs were treated with a final concentration of 1 μg/mL of the peptide pp65$_{495\text{-}503}$ (Anaspec, amino acid residues NLVPMVATV, catalog #: AS-28328) and 30 units/mL recombinant human IL-2 (PeproTech). For negative control treatment, PBMCs were treated with 30 units/mL recombinant human IL-2 (PeproTech) only. For expansion in 6-well G-REX plate format, 70E6 PBMCs were incubated in 5 mL supplemented media containing 7X concentrated pp65 (or test article) for 30 minutes prior to dilution to a final volume of 35 mL. For expansion in 24-well G-REX plate format, 5E6 PBMCs were incubated in 500 mL supplemented media containing 5X concentrated pp65 (or test article) for 30 minutes prior to dilution to a final volume of 2.5 mL.

For the cytotoxicity assays, 50 μL of assay medium containing RPMI 1640 media supplemented with 10% HI-FBS, 1% P/S, 50 μM 2-mercaptoethanol was added per well in a 96-well xCELLigence E plates (Agilent, part #5232368001). The E plates were loaded into the xCELLigence instrument (Agilent) under the conditions of 37°C and 5% CO2 for the baseline acquisition step. Next, NCI-H358 target cells were seeded at 1E4 per well in the E plates in an additional 100 μL volume per well of assay medium. The E plates were again loaded into xCELLigence for monitoring of net cellular adhesion on a per well basis. Following 24-hour incubation, the E plates were temporarily removed from the xCELLigence instrument for addition of the PBMCs and test articles. Briefly, 1E5 PBMCs were added to each well in additional volume of 50 μL per well. Similarly, test articles were added to each well in additional volume of 50 μL per well and the E plates were returned to xCELLigence for 48 hours of additional monitoring. The one-pot expansion and killing assays were conducted using methods analogous to those described previously albeit with several distinctions. Briefly, NCI-H358 cells were seeded at a density 2.5 -5E3 cells per well. The test article treated co-culture of culture of PBMCs and cancer cells were incubated at 37°C and 5% CO2 for 14 days with monitoring by xCELLigence.

Flow cytometry analyses for T cell activation and tetramer staining

For T cell activation assessment, PBMCs were transferred to a round-bottom 96-well plate and washed twice with fluorescence-activated cell sorting (FACS) buffer (PBS, pH 7.2, 2% HI-FBS, 2 mM ethylenediaminetetraacetic acid, and 0.01% sodium azide). The cells were then labeled for 30 minutes at 4°C in a FACS buffer solution containing 6-diamidino-2-phenylindole (DAPI, Life Technologies), anti-CD4-FITC (clone RPA-T4, Biolegend), anti-CD2-PE-Cy7 (clone RPA-2.10, Biolegend), anti-CD25-PE (clone M-A251, Biolegend), and

anti-CD69-APC (clone FN50, Biolegend), Fc receptor blocking reagent Human TruStain FcX (Biolegend). The cells were then washed twice in FACS buffer. All centrifugation steps were carried out at 400 g for 3 minutes. Labeled PBMC samples were assessed by flow cytometry using a FACSymphony instrument (Becton Dickinson) and the data were analyzed using FlowJo. T cell activation was determined as the percentage of live $CD25^+CD69^+CD4^+$ (or CD8+) cells among the total live CD4+ (or CD8+) cells.

For tetramer staining, the tetramers were prepared in-house. Briefly, streptavidin R-phycoerythrin (R-PE, Jackson ImmunoResearch) was added stepwise to 200 µg biotinylated pMHC monomer (pp65 – HLA-A*02:01) every 10 minutes across 10-time intervals, at a final ratio (binding sites: biotin) of 1:1. The tetramer preparation was conducted at room temperature, protected from light. For tetramer staining, the cells were labeled for 30 minutes at 4°C in a FACS buffer solution containing DAPI (Life Technologies), anti-CD8-FITC (clone SK1, Biolegend), anti-CD3-APC (clone OKT3, Biolegend), R-PE tetramer and Human TruStain FcX (Biolegend). Labeled cell samples were assessed by flow cytometry using a FACSymphony instrument (Becton Dickinson) and the data were analyzed using FlowJo.

Cytokine release assessment

Co-culture supernatants were thawed on ice and then examined for pro-inflammatory cytokine levels using a custom ProcartaPlex Human, NHP, and Canine Mix & Match Panels Luminex Kit (ThermoFisher Scientific) according to manufacturer's instruction. Supernatant (50 µl volume each) was transferred to the assay plate. Upon addition of the Read buffer the plate was read on Bio-Plex 3D Suspension Array System (Bio-Rad) and cytokine concentrations were calculated using Luminex xPONENT software. Data were analyzed and plotted using GraphPad Prism v 9.4.0.

In vitro T cell expansion specificity assays

Whole PBMCs from HLA-A*02:01+healthy CMV+ donors were cultured in complete RPMI/AIM-V medium (RPMI/AIM-V + 5% human A/B serum + 1% P/S) in the presence of GPS or IL-2-armored GPS molecules at concentrations of 25, 5, 1, and 0.2 nM in 24-well G-Rex plate (NC1000861, Wilson Wolf) for a period of 10–11 days. As a positive control, PBMCs were pulsed with 1 µg/mL of $CMVpp65_{495\text{-}503}$ peptide (NLVPMVATV, SP0010, MBL) and 1.6 nM IL-2 (HIL2-RO, Roche). As negative controls, PBMCs were cultured with PRAME-GPS or Fab/Fc IL-2 versions of PRAME-GPS. Abundance and the differentiation status of CMVpp65-specific and nonspecific CD8+ T cells, NK, Tregs and conventional $CD4^+$ T cells were assessed on days 0 and 10 of the expansion. CMVpp65-specific and nonspecific CD8+ T cells were identified as HLA-A*02:01CMVpp65 $Tetramer^+$ $CD8^+$ and HLA-A *02:01CMVpp65 Tetramer-CD8+, respectively. NK cells, Tregs and conventional CD4+ T cells were identified as $CD3^-CD56^{high/dim}$, CD4+CD25+CD127^{low} and CD4+CD25±, respectively. To characterize the differentiation phenotype of *T*- cells, baseline (day 0) and day 10 cultured PBMCs were stained with HLA-A*02:01CMVpp65 Tetramer,

anti-human CD8, anti-human CCR7 and anti-CD45RA antibodies. Based on these markers, T cells were classified as Naïve (T_{naive}; CCR7+CD45RA+), TCM (CCR7-CD45RA-), TEM (CCR7-CD45RA-) and TEMRA (CCR7-CD45RA+) subsets among CMV-specific and nonspecific CD8+ T cells.

In vivo *mouse model studies*

For the *in vivo* PK study, female Tg32 mice ($n = 3$ per group) were treated with 5 mg/kg of test article (GPS, Fab IL-2 GPS, and Fc IL-2 GPS) via single intravenous dose. Sera was collected at 6-time points, *i.e.*, 1, 24, 96, 264, 504, and 840 hours. Human antibody level in the mouse serum was measured by a universal ELISA method.

For the *in vivo* expansion study, female NSG mice (NOD.Cg-$Prkdc^{scid}IL$-$2Rg^{tm1Wjl}$/SzJ) aged 6 to 8 weeks ($n = 10$ per group) were purchased from Jackson Laboratory and housed and cared for in accordance with the approved Institutional Animal Care and Use Committee protocol and guidelines. On day 0, non-tumor bearing mice were IV engrafted with 2e6 unstimulated PBMCs or 2e6 CMV+ CD8+s per mouse. Following 6 hours post engraftment, mice in the treatment groups received via intraperitoneal injection 1 mg/kg of the appropriate test article with 20 mg/kg anti-mouse CD16/32 Cone 2.4G2 (BioXcell, BE0307). Mice continued to receive doses on Day 3, 7, 10, and 14 for 5 treatments. On day 24 and day 31, blood was collected via submandibular lancet sticks and analyzed for expansion via tetramer staining and flow cytometry analysis.

All animals were cared for following federal, state, and local guidelines and all animal experiments were conducted in compliance with the Animal Research: Reporting of In Vivo Experiments guidelines.

Deep sequencing of sorted CMV tetramer+ TCRβ CDR3 repertoires

Sorted CMV tetramer+ TCRβ CDR3 repertoires from six donors, pre-expanded via 1 µg/mL pp65 and 30 Units/mL IL-2 for 14 days, was isolated using the Zymo Quick RNA MicroPrep kit (Zymo Research, Cat#R1050) and quantified by NanoDrop. First-strand cDNA synthesis and TCR alpha and beta chain amplification were performed separately using the SMARTer Human TCR α/β Profiling Kit (Takara, Cat#635014). Illumina sequence adapters and unique HT indexes were added to β amplicons of each donor in the final semi-nested PCR to allow for NGS and demultiplexing. PCR products were gel purified on a 2% agarose gel. The final libraries were quantified by Qubit dsDNA HS assay (ThermoFisher) and their molecular sizes were determined by Tapestation D1000 assay on a Tapestation 4200 (Agilent). After equimolar concentrations of libraries were pooled together, sequencing and data demultiplexing was performed on an Illumina MiSeq sequencer with a V3 flow cell and 2X300bp paired-end reading. An average of 4 million reads were obtained for each sample.

For analysis of fastq files, for each sample, paired end reads were merged using fastp[71] (version 0.20.1) using correction over paired region (*Command 1*). The resulting fasta files were passed through a simple custom program to trim-off the first and last 8

bps to remove artificial variation introduced during priming, and then the resulting output was then de-duplicated using vsearch[72] (v2.14.2), incorporating count into fasta header (*Command 2*). Fasta sequences were then filtered (*Filter set 1*) to remove any sequences containing ambiguous base calls (N) using a custom script and then run through Igblastn[72] (v1.16.0 from igblast package 1.17.0) against IMGT germlines (202049–2 (1 December 2020)) to enable the extraction of CDR3 sequences. The output of which was then parsed with a shell script to extract the initial vsearch count (unique DNA replicate count) and the CDR3 sequences to generate a table of three columns (Sample name, Count, CDR3). Lastly, the sequences were further aggregated on unique CDR3 amino acid sequences by adding together the unique DNA replicate counts for each CDR3 as detailed in Supplementary Table S1. Sequences occurring in at least two donors and at least 10 times per donor were selected for multiple sequence alignment and phylogenetic analysis via Clustal Omega.

Command 1: fastp – merge -i <inputpath>R1_001.fastq.gz -I inputpath>R2_001.fastq.gz -w 6 -c – merged_out <outpath>merged.fa – out1 <outpath>R1.orphan – out2 <outpath>R2.orphan – unpaired1 <outpath>R1.unpaired – unpaired2 <outpath>R2.unpaired

Command 2: vsearch – derep_fulllength <input.fa> –output <output.fa> –sizeout – fasta_width 0

Filter set 1: igblastn -germline_db_V TRV.fasta -germline_db_D TRD.fasta -germline_db_J TRJ.fasta -auxiliary_data optional_file/human_gl.aux -ig_seqtype TCR -organism human -domain_system imgt -num_alignments_V 1 -num_alignments_D 1 -num_alignments_J 1 -outfmt 19 -query –

Data analysis, in silico protein modeling and statistical analysis

Data and statistical analyses were performed using Prism 9.5.1.733 (GraphPad). Curve fitting and EC_{50} value determination was performed by non-linear regression. Significant differences were determined by one-way ANOVA followed by Tukey multiple comparisons test and paired t-test as specified. Statistical significance was accepted for *p* values < 0.05 at 95% confidence interval. For Octet, kinetic analyses were performed using Octet 384 software (v.7.2) with a global fit and 1:1 binding model, with Pearson's Chi-squared test less than 5. For *in silico* protein modeling, protein lobes were modeled using ESMfold (Evolutionary Scale Modeling) and arranged based on linker length, flexibility and minimal steric hindrance. The loops were built manually by coot with local simulation, and the graphics were produced using PyMol.

Funding

Abbreviations

CMV	cytomegalovirus
DSF	differential scanning fluorimetry
EBV	Epstein-Barr virus
EGFR	epidermal growth factor receptor
Fab	antigen-binding fragment
GPS	guided-pMHC-staging
HLA	human leukocyte antigen
IL-2	interleukin-2
LC-MS	liquid chromatography-mass spectrometry
mAb	monoclonal antibody
NK	natural killer
PBMCs	peripheral blood mononuclear cells
PK	pharmacokinetics
pMHC	peptide-major histocompatibility class I
pMHC-IgGs	peptide-major histocompatibility class I bispecific antibodies
POC	proof-of-concept
pp65	CMV-specific nonameric peptide pp65$_{495-503}$
PRAME	preferentially expressed antigen in melanoma
TAA	tumor-associated antigen
TCE	T cell engager
TI	therapeutic index
Tm	melting temperature
TME	tumor microenvironment
Treg	regulatory T cell

Acknowledgments

Disclosure statement

No potential conflict of interest was reported by the author(s).

Authors contributions

J.S.S., E.W. and Y.M. designed the research. J.S.S., K.L., W.L., F.H., P.S., C.Y., J.L. and K.A. cloned, expressed and purified the antibodies. H.Z. conducted *in silico* protein modeling. Y.G. conducted LCMS analyses. J.S.S. and K.L. conducted Octet binding analyses. A.D. conducted developability analyses. X.C., P.P., J.D. and Y.W. conducted the in vivo PK assay. J.S.S., K.L., C.Y., P.S., V.C., HC.C., S.D., S.C., E.W. and Y.M. designed/conducted *in vitro* biological activity assays. C.R.K., K.M., and S.P. conducted the *in vivo* efficacy study. C.Z., E.W. C.H., M.K., Y.S., J.S.S, and H.Z. conducted the NGS study and subsequent analyses. J.S. S. and E.W. wrote the manuscript with input from the coauthors. K.L., C.Y. and Y.M. edited and revised the manuscript.

References

1. Vafa O, Nd T. Perspective: designing T-Cell engagers with better Therapeutic windows. Front Oncol. 2020;10:446. doi:10.3389/fonc.2020.00446. PMID: 32351885.
2. Zhou S, Liu M, Ren F, Meng X, Yu J. The landscape of bispecific T cell engager in cancer treatment. Biomark Res. 2021;9:38. doi:10.1186/s40364-021-00294-9. PMID: 34039409.
3. Shanshal M, Caimi PF, Adjei AA, Ma WW. T-Cell engagers in solid cancers-current landscape and future directions. Cancers (Basel). 2023;15. doi:10.3390/cancers15102824. PMID: 37345160.
4. The antibody society. Therapeutic monoclonal antibodies approved or in regulatory review. 2024 Aug 16; www.antibodysociety.org/antibody-therapeutics-product-data.

5. Singh A, Dees S, Grewal IS. Overcoming the challenges associated with CD3+ T-cell redirection in cancer. Br J Cancer. 2021;124:1037–48. doi:10.1038/s41416-020-01225-5. PMID: 33469153.

6. Ball K, Dovedi SJ, Vajjah P, Phipps A. Strategies for clinical dose optimization of T cell-engaging therapies in oncology. MAbs. 2023;15:2181016. doi:10.1080/19420862.2023.2181016. PMID: 36823042.

7. Dang K, Castello G, Clarke SC, Li Y, Balasubramani A, Boudreau A, Davison L, Harris KE, Pham D, Sankaran P. et al. Attenuating CD3 affinity in a PSMAxCD3 bispecific antibody enables killing of prostate tumor cells with reduced cytokine release. J Immunother Cancer. 2021;9. doi:10.1136/jitc-2021-002488. PMID: 34088740.

8. Poussin M, Sereno A, Wu X, Huang F, Manro J, Cao S, Carpenito C, Glasebrook A, Powell DJ Jr., Demarest S. Dichotomous impact of affinity on the function of T cell engaging bispecific antibodies. J Immunother Cancer. 2021;9(7). doi:10.1136/jitc-2021-002444. PMID: 34253637.

9. Staflin K, Zuch de Zafra CL, Schutt LK, Clark V, Zhong F, Hristopoulos M, Clark R, Li J, Mathieu M, Chen X. et al. Target arm affinities determine preclinical efficacy and safety of anti-HER2/CD3 bispecific antibody. JCI Insight. 2020;5. doi:10.1172/jci.insight.133757. PMID: 32271166.

10. Mandikian D, Takahashi N, Lo AA, Li J, Eastham-Anderson J, Slaga D, Ho J, Hristopoulos M, Clark R, Totpal K. et al. Relative target affinities of T-Cell-dependent bispecific antibodies determine biodistribution in a solid tumor mouse Model. Mol Cancer Ther. 2018;17:776–85. doi:10.1158/1535-7163.MCT-17-0657. PMID: 29339550.

11. Ellerman D. Bispecific T-cell engagers: towards understanding variables influencing the in vitro potency and tumor selectivity and their modulation to enhance their efficacy and safety. Methods. 2019;154:102–17. doi:10.1016/j.ymeth.2018.10.026. PMID: 30395966.

12. Rosato PC, Wijeyesinghe S, Stolley JM, Nelson CE, Davis RL, Manlove LS, Pennell CA, Blazar BR, Chen CC, Geller MA. et al. Virus-specific memory T cells populate tumors and can be repurposed for tumor immunotherapy. Nat Commun. 2019;10:567. doi:10.1038/s41467-019-08534-1. PMID: 30718505.

13. Poon MML, Byington E, Meng W, Kubota M, Matsumoto R, Grifoni A, Weiskopf D, Dogra P, Lam N, Szabo PA. et al. Heterogeneity of human anti-viral immunity shaped by virus, tissue, age, and sex. Cell Rep. 2021;37(9):110071. doi:10.1016/j.celrep.2021.110071. PMID: 34852222.

14. Hosie L, Pachnio A, Zuo J, Pearce H, Riddell S, Moss P. Cytomegalovirus-specific T cells restricted by HLA-Cw*0702 increase markedly with age and dominate the CD8. Front Immunol. 2017;8:1776. doi:10.3389/fimmu.2017.01776. PMID: 29312307.

15. Nauclér CS, Geisler J, Vetvik K. The emerging role of human cytomegalovirus infection in human carcinogenesis: a review of current evidence and potential therapeutic implications. Oncotarget. 2019;10:4333–47. doi:10.18632/oncotarget.27016. PMID: 31303966.

16. El Baba R, Herbein G. Immune landscape of CMV infection in cancer patients: from "Canonical" diseases toward virus-elicited Oncomodulation. Front Immunol. 2021;12:730765. doi:10.3389/fimmu.2021.730765. PMID: 34566995.

17. Schmittnaegel M, Hoffmann E, Imhof-Jung S, Fischer C, Drabner G, Georges G, Klein C, Knoetgen H. A new class of bifunctional Major histocompatibility class I antibody fusion molecules to redirect CD8 T cells. Mol Cancer Ther. 2016;15(9):2130–42. doi:10.1158/1535-7163.MCT-16-0207. PMID: 27353170.

18. Schmittnaegel M, Levitsky V, Hoffmann E, Georges G, Mundigl O, Klein C, Knoetgen H. Committing cytomegalovirus-specific CD8 T cells to eliminate tumor cells by bifunctional Major histocompatibility class I antibody fusion molecules. Cancer Immunol Res. 2015;3(7):764–76. doi:10.1158/2326-6066.CIR-15-0037. PMID: 25691327.

19. Fischer C, Munks MW, Hill AB, Kroczek RA, Bissinger S, Brand V, Schmittnaegel M, Imhof-Jung S, Hoffmann E, Herting F. et al. Vaccine-induced CD8 T cells are redirected with peptide-mhc class I-IgG antibody fusion proteins to eliminate tumor cells in vivo. MAbs. 2020;12:1834818. doi:10.1080/19420862.2020.1834818. PMID: 33151105.

20. Britsch I, van Wijngaarden Ap, Ke X, Majm H, Samplonius DF, Ploeg EM, Helfrich W. Novel fab-peptide-HLA-I fusion proteins for redirecting pre-existing anti-cmv T cell immunity to selective eliminate carcinoma cells. Oncoimmunology. 2023;12:2207868. doi:10.1080/2162402X.2023.2207868. PMID: 37180637.

21. Jung K, Son M-J, Lee S-Y, Kim J-A, D-H K, Yoo S, Kim C-H, Kim Y-S. Antibody-mediated delivery of a viral MHC-I epitope into the cytosol of target tumor cells repurposes virus-specific CD8 + T cells for cancer immunotherapy. Mol Cancer. 2022;21:1–20. doi:10.1186/s12943-022-01574-0.

22. Bachmann MF, Oxenius A. Interleukin 2: from immunostimulation to immunoregulation and back again. EMBO Rep. 2007;8:1142–48. doi:10.1038/sj.embor.7401099. PMID: 18059313.

23. Raeber ME, Sahin D, Karakus U, Boyman O. A systematic review of interleukin-2-based immunotherapies in clinical trials for cancer and autoimmune diseases. EBioMedicine. 2023;90:104539. doi:10.1016/j.ebiom.2023.104539. PMID: 37004361.

24. Merani S, Pawelec G, Kuchel GA, McElhaney JE. Impact of aging and cytomegalovirus on immunological response to influenza vaccination and infection. Front Immunol. 2017;8:784. doi:10.3389/fimmu.2017.00784. PMID: 28769922.

25. Staras SA, Dollard SC, Radford KW, Flanders WD, Pass RF, Cannon MJ. Seroprevalence of cytomegalovirus infection in the United States, 1988-1994. Clin Infect Dis. 2006;43:1143–51. doi:10.1086/508173. PMID: 17029132.

26. Fowler K, Mucha J, Neumann M, Lewandowski W, Kaczanowska M, Grys M, Schmidt E, Natenshon A, Talarico C, Buck PO. et al. A systematic literature review of the global seroprevalence of cytomegalovirus: possible implications for treatment, screening, and vaccine development. BMC Public Health. 2022;22:1659. doi:10.1186/s12889-022-13971-7. PMID: 36050659.

27. Bate SL, Dollard SC, Cannon MJ. Cytomegalovirus seroprevalence in the United States: the national health and nutrition examination surveys, 1988-2004. Clin Infect Dis. 2010;50(11):1439–47. doi:10.1086/652438. PMID: 20426575.

28. Cannon MJ, Schmid DS, Hyde TB. Review of cytomegalovirus seroprevalence and demographic characteristics associated with infection. Rev Med Virol. 2010;20(4):202–13. doi:10.1002/rmv.655. PMID: 20564615.

29. Wang B, Yang C, Jin X, Du Q, Wu H, Dall'acqua W, Mazor Y. Regulation of antibody-mediated complement-dependent cytotoxicity by modulating the intrinsic affinity and binding valency of IgG for target antigen. MAbs. 2020;12:1690959. doi:10.1080/19420862.2019.1690959. PMID: 31829766.

30. Mazor Y, Yang C, Borrok MJ, Ayriss J, Aherne K, Wu H, Dall'acqua WF. Enhancement of immune effector functions by modulating IgG's intrinsic affinity for target antigen. PLoS One. 2016;11:e0157788. doi:10.1371/journal.pone.0157788. PMID: 27322177.

31. Mazor Y, Sachsenmeier KF, Yang C, Hansen A, Filderman J, Mulgrew K, Wu H, Dall'acqua WF. Enhanced tumor-targeting selectivity by modulating bispecific antibody binding affinity and format valence. Sci Rep. 2017;7:40098. doi:10.1038/srep40098. PMID: 28067257.

32. Mazor Y, Oganesyan V, Yang C, Hansen A, Wang J, Liu H, Sachsenmeier K, Carlson M, Gadre DV, Borrok MJ. et al. Improving target cell specificity using a novel monovalent bispecific IgG design. MAbs. 2015;7:377–89. doi:10.1080/19420862.2015.1007816. PMID: 25621507.

33. Mazor Y, Hansen A, Yang C, Chowdhury PS, Wang J, Stephens G, Wu H, Dall'acqua WF. Insights into the molecular basis of a bispecific antibody's target selectivity. MAbs. 2015;7:461–69. doi:10.1080/19420862.2015.1022695. PMID: 25730144.

34. Dovedi SJ, Elder MJ, Yang C, Sitnikova SI, Irving L, Hansen A, Hair J, Jones DC, Hasani S, Wang B. et al. Design and efficacy of a monovalent bispecific PD-1/CTLA4 antibody that enhances CTLA4 blockade on PD-1. Cancer Discov. 2021;11:1100–17. doi:10.1158/2159-8290.CD-20-1445. PMID: 33419761.

35. Gerdes CA, Nicolini VG, Herter S, van Puijenbroek E, Lang S, Roemmele M, Moessner E, Freytag O, Friess T, Ries CH. et al. GA201 (RG7160): a novel, humanized, glycoengineered anti-egfr antibody with enhanced ADCC and superior in vivo efficacy compared with cetuximab. Clin Cancer Res. 2013;19(5):1126–38. doi:10.1158/1078-0432.CCR-12-0989. PMID: 23209031.

36. Solberg OD, Mack SJ, Lancaster AK, Single RM, Tsai Y, Sanchez-Mazas A, Thomson G. Balancing selection and heterogeneity across the classical human leukocyte antigen loci: a meta-analytic review of 497 population studies. Hum Immunol. 2008;69 (7):443–64. doi:10.1016/j.humimm.2008.05.001. PMID: 18638659.

37. Soto-Nava M, Avila-Ríos S, Valenzuela-Ponce H, García-Morales C, Carlson JM, Tapia-Trejo D, Garrido-Rodriguez D, Alva-Hernández SN, García-Tellez TA, Murakami-Ogasawara A. et al. Weaker HLA footprints on HIV in the unique and highly genetically admixed Host population of Mexico. J Virol. 2018;92. doi:10.1128/JVI.01128-17. PMID: 29093100.

38. Jawdat D, Uyar FA, Alaskar A, Müller CR, Hajeer A. HLA-A, -B, -C,-DRB1, -DQB1, and -DPB1 allele and haplotype frequencies of 28,927 Saudi stem cell donors typed by next-generation sequencing. Front Immunol. 2020;11:544768. doi:10.3389/fimmu.2020.544768. PMID: 33193311.

39. Quayle SN. CUE-101, a novel E7-pHLA-IL2-Fc fusion protein, enhances tumor antigen-specific T-Cell activation for the treatment of HPV16-driven malignancies | clinical cancer research |. American Association for Cancer Research; 2023. doi:10.1158/1078-0432.CCR-19-3354.

40. Vita N, Magazin M, Marchese E, Lupker J, Ferrara P. Closely related glycosylation patterns of recombinant human IL-2 expressed in a CHO cell line and natural IL-2. Lymphokine Res. 1990;9:67–79. https://www.ncbi.nlm.nih.gov/pubmed/2109157. PMID: 2109157.

41. Mieczkowski C, Zhang X, Lee D, Nguyen K, Lv W, Wang Y, Zhang Y, Way J, Gries JM. Blueprint for antibody biologics developability. MAbs. 2023;15(1):2185924. doi:10.1080/19420862.2023.2185924. PMID: 36880643.

42. Spolski R, Li P, Leonard WJ. Biology and regulation of IL-2: from molecular mechanisms to human therapy. Nat Rev Immunol. 2018;18(10):648–59. doi:10.1038/s41577-018-0046-y. PMID: 30089912.

43. Driesen J, Popov A, Schultze JL. CD25 as an immune regulatory molecule expressed on myeloid dendritic cells. Immunobiology. 2008;213(9–10):849–58. doi:10.1016/j.imbio.2008.07.026. PMID: 18926299.

44. Seidel RD, Merazga Z, Thapa DR, Soriano J, Spaulding E, Vakkasoglu AS, Ruthardt P, Bautista W, Quayle SN, Kiener PA. et al. Peptide-hla-based immunotherapeutics platforms for direct modulation of antigen-specific T cells. Sci Rep. 2021; 11. doi:10.1038/s41598-021-98716-z.

45. Li M, Garforth SJ, O'Connor KE, Su H, Lee DM, Celikgil A, Chaparro RJ, Seidel RD, Jones RB, Arav-Boger R. et al. T cell receptor–targeted immunotherapeutics drive selective in vivo HIV- and cmv-specific T cell expansion in humanized mice. J Clin Investigation. 2021; 131. doi:10.1172/jci141051.

46. Del Campo Ab, Kyte JA, Carretero J, Zinchencko S, Méndez R, González-Aseguinolaza G, Ruiz-Cabello F, Aamdal S, Gaudernack G, Garrido F. et al. Immune escape of cancer cells with beta2-microglobulin loss over the course of metastatic melanoma. Int J Cancer. 2014;134:102–13. doi:10.1002/ijc.28338. PMID: 23784959.

47. Pereira C, Gimenez-Xavier P, Pros E, Pajares MJ, Moro M, Gomez A, Navarro A, Condom E, Moran S, Gomez-Lopez G. et al. Genomic profiling of patient-derived xenografts for lung cancer identifies B2M inactivation impairing immunorecognition. Clin Cancer Res. 2017;23(12):3203–13. doi:10.1158/1078-0432.CCR-16-1946. PMID: 28302866.

48. Gettinger S, Choi J, Hastings K, Truini A, Datar I, Sowell R, Wurtz A, Dong W, Cai G, Melnick MA. et al. Impaired HLA class I antigen processing and presentation as a mechanism of acquired resistance to immune checkpoint inhibitors in lung cancer. Cancer Discov. 2017;7(12):1420–35. doi:10.1158/2159-8290.CD-17-0593. PMID: 29025772.

49. Dhatchinamoorthy K, Colbert JD, Rock KL. Cancer immune evasion through Loss of MHC class I antigen presentation. Front Immunol. 2021;12:636568. doi:10.3389/fimmu.2021.636568. PMID: 33767702.

50. Watson NF, Ramage JM, Madjd Z, Spendlove I, Ellis IO, Scholefield JH, Durrant LG. Immunosurveillance is active in colorectal cancer as downregulation but not complete loss of MHC class I expression correlates with a poor prognosis. Int J Cancer. 2006;118:6–10. doi:10.1002/ijc.21303. PMID: 16003753.

51. Koopman LA, Corver WE, van der Slik Ar, Giphart MJ, Fleuren GJ. Multiple genetic alterations cause frequent and heterogeneous human histocompatibility leukocyte antigen class I loss in cervical cancer. J Exp Med. 2000;191:961–76. doi:10.1084/jem.191.6.961. PMID: 10727458.

52. Wang H, Liu B, Wei J. Beta2-microglobulin(B2M) in cancer immunotherapies: biological function, resistance and remedy. Cancer Lett. 2021;517:96–104. doi:10.1016/j.canlet.2021.06.008. PMID: 34129878.

53. Hazini A, Fisher K, Seymour L. Deregulation of HLA-I in cancer and its central importance for immunotherapy. J Immunother Cancer. 2021; 9. doi:10.1136/jitc-2021-00289. PMID: 34353849.

54. Wooldridge L, van den Berg HA, Glick M, Gostick E, Laugel B, Hutchinson SL, Milicic A, Brenchley JM, Douek DC, Price DA. et al. Interaction between the CD8 coreceptor and major histocompatibility complex class I stabilizes T cell receptor-antigen complexes at the cell surface. J Biol Chem. 2005;280:27491–501. doi:10.1074/jbc.M500555200. PMID: 15837791.

55. Mortara L, Balza E, Bruno A, Poggi A, Orecchia P, Carnemolla B. Anti-cancer therapies employing IL-2 cytokine tumor targeting: contribution of innate, adaptive and immunosuppressive cells in the anti-tumor efficacy. Front Immunol. 2018;9:2905. doi:10.3389/fimmu.2018.02905. PMID: 30619269.

56. Den Otter W, Jacobs JJ, Battermann JJ, Hordijk GJ, Krastev Z, Moiseeva EV, Stewart RJ, Ziekman PG, Koten JW. Local therapy of cancer with free IL-2. Cancer Immunol Immunother. 2008;57 (7):931–50. doi:10.1007/s00262-008-0455-z. PMID: 18256831.

57. Nagatani M, Kodera T, Suzuki D, Igura S, Fukunaga Y, Kanemitsu H, Nakamura D, Mochizuki M, Kemi M, Tamura K. et al. Comparison of biological features between severely immuno-deficient NOD/Shi-scid Il2rg. Exp Anim. 2019;68:471–82. doi:10.1538/expanim.19-0024. PMID: 31118345.

58. Thome JJ, Farber DL. Emerging concepts in tissue-resident T cells: lessons from humans. Trends Immunol. 2015;36(7):428–35. doi:10.1016/j.it.2015.05.003. PMID: 26072286.

59. Snyder CM. Buffered memory: a hypothesis for the maintenance of functional, virus-specific CD8(+) T cells during cytomegalovirus infection. Immunol Res. 2011;51(2–3):195–204. doi:10.1007/s12026-011-8251-9. PMID: 22058020.

60. Wills MR, Carmichael AJ, Mynard K, Jin X, Weekes MP, Plachter B, Sissons JG. The human cytotoxic T-lymphocyte (CTL) response to cytomegalovirus is dominated by structural protein pp65: frequency, specificity, and T-cell receptor usage of pp65-specific CTL. J Virol. 1996;70:7569–79. doi:10.1128/JVI.70.11.7569-7579.1996. PMID: 8892876.

61. Gratama JW, Brooimans RA, van der Holt B, Sintnicolaas K, van Doornum G, Niesters HG, Löwenberg B, Cornelissen JJ. Monitoring cytomegalovirus IE-1 and pp65-specific CD4+ and CD8+ T-cell responses after allogeneic stem cell transplantation may identify patients at risk for recurrent CMV reactivations.

Cytometry B Clin Cytom. 2008;74(4):211–20. doi:10.1002/cyto.b.20420. PMID: 18454493.

62. Peggs KS, Thomson K, Samuel E, Dyer G, Armoogum J, Chakraverty R, Pang K, Mackinnon S, Lowdell MW. Directly selected cytomegalovirus-reactive donor T cells confer rapid and safe systemic reconstitution of virus-specific immunity following stem cell transplantation. Clin Infect Dis. 2011;52(1):49–57. doi:10.1093/cid/ciq042. PMID: 21148519.

63. Schuessler A, Smith C, Beagley L, Boyle GM, Rehan S, Matthews K, Jones L, Crough T, Dasari V, Klein K. et al. Autologous T-cell therapy for cytomegalovirus as a consolidative treatment for recurrent glioblastoma. Cancer Res. 2014;74:3466–76. doi:10.1158/0008-5472.CAN-14-0296. PMID: 24795429.

64. Derhovanessian E, Maier AB, Hähnel K, Beck R, de Craen Ajm, Slagboom EP, Westendorp RGJ, Pawelec G. Infection with cytomegalovirus but not herpes simplex virus induces the accumulation of late-differentiated CD4+ and CD8+ T-cells in humans. J Gen Virol. 2011;92:2746–56. doi:10.1099/vir.0.036004-0. PMID: 21813708.

65. Wills MR, Okecha G, Weekes MP, Gandhi MK, Sissons PJ, Carmichael AJ. Identification of naive or antigen-experienced human CD8(+) T cells by expression of costimulation and chemokine receptors: analysis of the human cytomegalovirus-specific CD8(+) T cell response. J Immunol. 2002;168:5455–64. doi:10.4049/jimmunol.168.11.5455. PMID: 12023339.

66. Becher LRE, Nevala WK, Sutor SL, Abergel M, Hoffmann MM, Parks CA, Pease LR, Schrum AG, Markovic SN, Gil D. Public and private human T-cell clones respond differentially to HCMV antigen when boosted by CD3 copotentiation. Blood Adv. 2020;4 (21):5343–56. doi:10.1182/bloodadvances.2020002255. PMID: 33125463.

67. Trautmann L, Rimbert M, Echasserieau K, Saulquin X, Neveu B, Dechanet J, Cerundolo V, Bonneville M. Selection of T cell clones expressing high-affinity public TCRs within human cytomegalovirus-specific CD8 T cell responses. J Immunol. 2005;175(9):6123–32. doi:10.4049/jimmunol.175.9.6123. PMID: 16237109.

68. Kravtsov DS, Erbe AK, Sondel PM, Rakhmilevich AL. Roles of CD4+ T cells as mediators of antitumor immunity. Front Immunol. 2022;13:972021. doi:10.3389/fimmu.2022.972021. PMID: 36159781.

69. Accogli T, Bruchard M, Végran F. Modulation of CD4 T cell response according to tumor cytokine microenvironment. Cancers (Basel). 2021;13. doi:10.3390/cancers13030373. PMID: 33498483.

70. Shan L, Mody N, Sormani P, Rosenthal KL, Damschroder MM, Esfandiary R. Developability assessment of engineered monoclonal antibody variants with a complex self-association behavior using complementary analytical and in silico tools. Mol Pharm. 2018;15:5697–710. doi:10.1021/acs.molpharmaceut.8b00867. PMID: 30395473.

71. Chen S, Zhou Y, Chen Y, Gu J. Fastp: an ultra-fast all-in-one FASTQ preprocessor. Bioinformatics. 2018;34:i884–90. doi:10.1093/bioinformatics/bty560. PMID: 30423086.

72. Rognes T, Flouri T, Nichols B, Quince C, Mahé F. VSEARCH: a versatile open source tool for metagenomics. PeerJ. 2016;4:e2584. doi:10.7717/peerj.2584. PMID: 27781170.